STANFORD REMOTE SENSING LABORATORY

TECHNICAL REPORT #70-1

"DETAILED GROUND STUDY OF 8 - 13 MICRON INFRARED IMAGERY, CARRIZO PLAINS, CALIFORNIA"

by
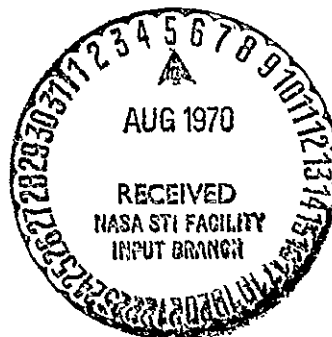
Robert W. Campbell, Jr.
Lawrence D. Hoover
Francisco Querol-Suñé

Graduate Students,
Departments of Geology and Geophysics
Stanford University
Stanford, California 94305

January 1970

REMOTE SENSING LABORATORY

SCHOOL OF EARTH SCIENCES

STANFORD UNIVERSITY ○ STANFORD, CALIFORNIA

STANFORD REMOTE SENSING LABORATORY

TECHNICAL REPORT #70-1

"DETAILED GROUND STUDY OF 8 - 13 MICRON INFRARED

IMAGERY, CARRIZO PLAINS, CALIFORNIA"

by

Robert W. Campbell, Jr.*

Lawrence D. Hoover**

Francisco Querol-Suñé

Graduate Students,

Departments of Geology and Geophysics

Stanford University

Stanford, California 94305

Approved: _____
                   R. J. P. Lyon
                   Principal Investigator

*presently with United States Coast Guard
**presently with NASA Manned Spacecraft Center, Houston, Texas

January 1970

STANFORD RSL TECHNICAL REPORT SERIES

Already Issued

67-1   "Field Infrared Analysis of Terrain-Spectral Correlation Program" Part I (by R. J. P. Lyon)

67-2   "Field Infrared Analysis of Terrain-Spectral Correlation Program" Part II and Part III (by R. J. P. Lyon)

67-3   "Statistical Analysis of IR Spectra--Stanford Programs Applied to USGS Spectra in Tech Letter #13 (by R. J. P. Lyon)

67-4   "Computer Reduction and Analysis of an Infrared Image" (by Keenan Lee)

68-1   "Infrared Exploration for Coastal and Shoreline Springs" (by Keenan Lee)

68-2   "Re-evaluation of the Normative Minerals of Sonora Pass Rock Standards-University of Nevada Reports #7 and #12" (by Attila· Kilinc)

68-3   Nearest Neighbor--A New Non-parametric Test Used for Classifying Spectral Data" (by Paul Switzer)

68-4   Final Report "Field Analysis of Terrain"--NGR-05-020-115 (contains all the drawings and logic diagrams for Stanford CVF Spectrometer and Digital Data Recording System (by R. J. P. Lyon)

69-1   "Mission 78--Flights 1 and 2 Ninety-Day Report" (by R. J. P. Lyon)

69-2   "Quantitative Geological Analysis of Multiband Photography from the Mono Craters Area, California" (by G. I. Ballew)

69-3   "The Stanford Infrared Spectra Processing Package" (by John Moore with subsequent modifications by Michael Heathman)

69-4   "Thermal Dynamics at the Earth-Air Interface: The Implications for Remote Sensing of the Geologic Environment" (by Rossman Smith)

69-5   "Infrared Spectrometry Studies: Final Report Phase I" (by R. J. P. Lyon)

69-6   "Infrared Spectrometry Studies: Final Report Phase II"
        (by R. J. P. Lyon and Attila Kilinc)

69-7   "Infrared Exploration for Shoreline Springs at Mono Lake,
        California, Test Site" (by Keenan Lee)   .

70-1   "Detailed Ground Study of 8-13 μm Infrared Imagery, Carrizo
        Plains, California" (by R. Campbell, Jr., L. D. Hoover, and
        F. Querol-Suñé)

70-2   "Terms in Geologic Remote Sensing; A Condensed Glossary"
        (by R. J. P. Lyon)

70-3   "Geologic Interpretation of Airborne Infrared Thermal Imagery
        of Goldfield, Nevada" (by I. A. Kilinc and R. J. P. Lyon)

70-4   "Surface Heat Flow Studies for Remote Sensing of Geothermal
        Resources" (by H. Hase, Geol. Survey of Japan)

70-5   "Geophysical Analysis of Termal Infrared Imagery near Gold-
        field, Nevada: Experimental and Correlation Analysis"
        (by W. B. Ervine)

70-6   "The Multiband Approach to Geologic Mapping from Orbiting
        Satellites: Is it Redundant or Vital?" (by R. J. P. Lyon) to
        be published by AIAA.

70-7   "Airborne Geological Mapping Using Infrared Emission Spectra"
        (by R. J. P. Lyon and J. Patterson) to be published in Proc.
        6th Remote Sensing Conference.

70-8   "Pseudo-Radar: Very High Contrast Aerial Photography at Low
        Sun Angles" (by R. J. P. Lyon, Jose Mercado, and Robt. Campbell
        Jr.) to be published in Photogrammetric Engineering.

70-9   "Remote Sensing in Exploration for Mineral Deposits"
        (by R. J. P. Lyon and Keenan Lee) to be published in Economic
        Geology.

ABSTRACT

A field study of the Carrizo Plains area, central California, was undertaken over a 48-hour period in May 31 - June 1, 1969, to check in detail, the causes of the dark (cold) thermal anomalies associated with the San Andreas Fault trace as previously detected 4 years earlier on thermal infrared (the 8-13 micron band) imagery (July 17, 1965). Radiometric and "contact" ground temperatures during these nights showed a strong negative correlation with moisture content of the near-surface soil. The original anomaly on the imagery was also redetected and further defined by these ground temperature measurements. The NE side of the fault trace had a higher soil moisture content, and a correspondingly lower temperature than the SW side. Radiometric temperatures were consistently lower than contact ground temperatures. Several effects are discussed, related to this variation. Humidity, topography, vegetation cover, and time of night influenced the temperatures obtained.

TABLE OF CONTENTS

GLOSSARY AND DEFINITIONS

Absolute humidity - The actual quantity or mass of water vapor present in a given volume of air, generally expressed in grains per cubic foot or in grams per cubic meter (Howell, 1960).

Cavity-type blackbody - Blackened, 15° conical cavity, water-temperature controlled with a mercury thermometer as the measuring element. The diameter of the aperture is one inch.

Contact temperature - Temperature measured with a thermometer or thermistor probe inserted into the target.

Emissivity - A special case of emittance, the fundamental property of a material that has an optically smooth surface and is sufficiently thick to be opaque (Wolfe, 1965).

Emittance - The ratio of the radiant energy emission from a body as a consequence of its temperature only, to the corresponding rate of emission from a blackbody at the same temperature (Wolfe, 1965).

Inter-layer water - Molecular water fixed between the layers in the crystal structure of a mineral.

Interstitial water - Pore water (or freely-flowing water) situated in the interstices or between the grain boundaries of the soil.

Radiant emittance - Radiant power per unit area emitted from a surface (Wolfe, 1965).

Radiometric temperature - Non-contact, infrared radiation temperature as measured with a radiation thermometer presuming the surface emits as a blackbody.

Relative humidity - The ratio of the actual amount of water vapor present, in the portion of the atmosphere under consideration, to the quantity which would be there if it were saturated (Howell, 1960).

Sky temperature - Temperature of the sky as measured with the radiation thermometer.

Soil moisture (percent) - Weight percent of water and volatile material lost by a soil when heated under vacuum conditions (10^{-5} torr) at 110° C.

Station-line - Imaginary straight line in the field, along which all of the stations are located.

Surface temperature - Contact temperature measured at the surface of the target.

Thermal anomaly - High contrast between gray tones in an infrared image.

Traverse - Continuous or discontinuous series of measurements along a station line.

LIST OF TABLES

LIST OF FIGURES

I. INTRODUCTION

Thermal infrared imagery, recording radiation of filtered 8 - 13μm wavelength, was flown by NASA Convair 240 aircraft on June 17, 1965, in the Carrizo Plains area of central California (Mission 10). Several strong (cold) thermal anomalies are observed along the main trace of the San Andreas Fault. No concurrent ground calibration data are available to help to explain most of these anomalies.

In 1966, the USGS published a preliminary report on this area on the use of this infrared imagery in the study of the San Andreas Fault system (R. E. Wallace and R. M. Moxham, 1966). They suggested that certain properties of soil and rock units such as "degree of compaction, platiness of surface fragments, and soil moisture may influence greatly the thermal inertia and emissivity and thus the surface temperature" of those materials. In order to assess the validity of these suggestions, a comprehensive field study was conducted to gather quantitative ground data on three of the most-pronounced thermal anomalies associated with the San Andreas Fault, as indicated on the thermal infrared imagery of the Carrizo Plains area. The numeric data has been analyzed by visual inspection (plotting) and by computer analysis.

II. LOCATION

The area of study is located on the eastern side of Carrizo Plains approximately 45 miles east of San Luis Obispo, California. Detailed work was carried out near the trace of the San Andreas Fault in Sections 17 through 20, T.30S, R.20E of the McKittrick Summit, California topographic quadrangle, approximately 4 miles NE of Soda Lake (see Fig. 1.).
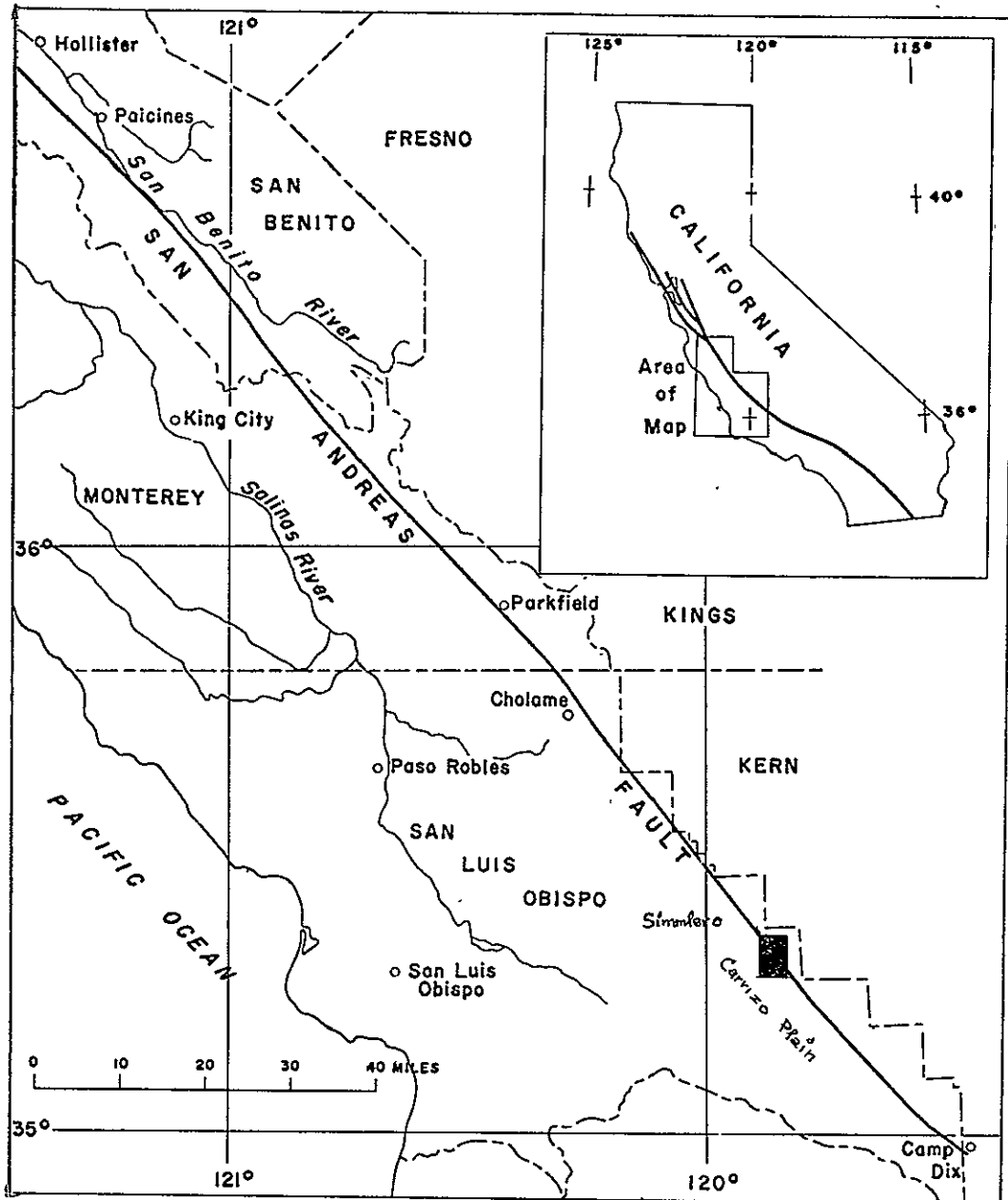
Figure 1 — Index map, showing approximate location of the
San Andreas Fault and the area of study.

(After Brown and Wallace, 1968)

3

III. GENERAL GEOLOGY OF THE AREA

The region was selected because several thermal anomalies existed
along the fault trace; the specific area under investigation was chosen
because there was no radical change in lithology in the sites of interest.
This would eliminate lithology as an independent variable. In addition,
it was readily accessible for truck-mounted instrumentation. Figure 2
is a geologic map of that area of Carrizo Plains in which the field
work was carried out. This is part of a larger map (as yet unpublished)
by T. W. Dibblee, Jr., completed in November 1968 for the National
Center for Earthquake Research of the USGS.

The two formations present in the area of the sites are Quaternary
alluvium (Qa), present on the NE side of the fault, and the Pliocene-
Pleistocene Paso Robles Formation (QTp), present on the SW side of the
fault.

The alluvium consists of unconsolidated sands, gravels, and silts
of Quaternary and Recent age. The Paso Robles Formation consists of
unconsolidated to semi-consolidated terrestrial gravels, sands, silts,
lacustrine clays and conglomerates of Pliocene-Pleistocene age. It
forms slight topographic ridges paralleling the fault and approximately
20 to 40 feet high, while the alluvium covers the broad, low-relief,
valley floor.
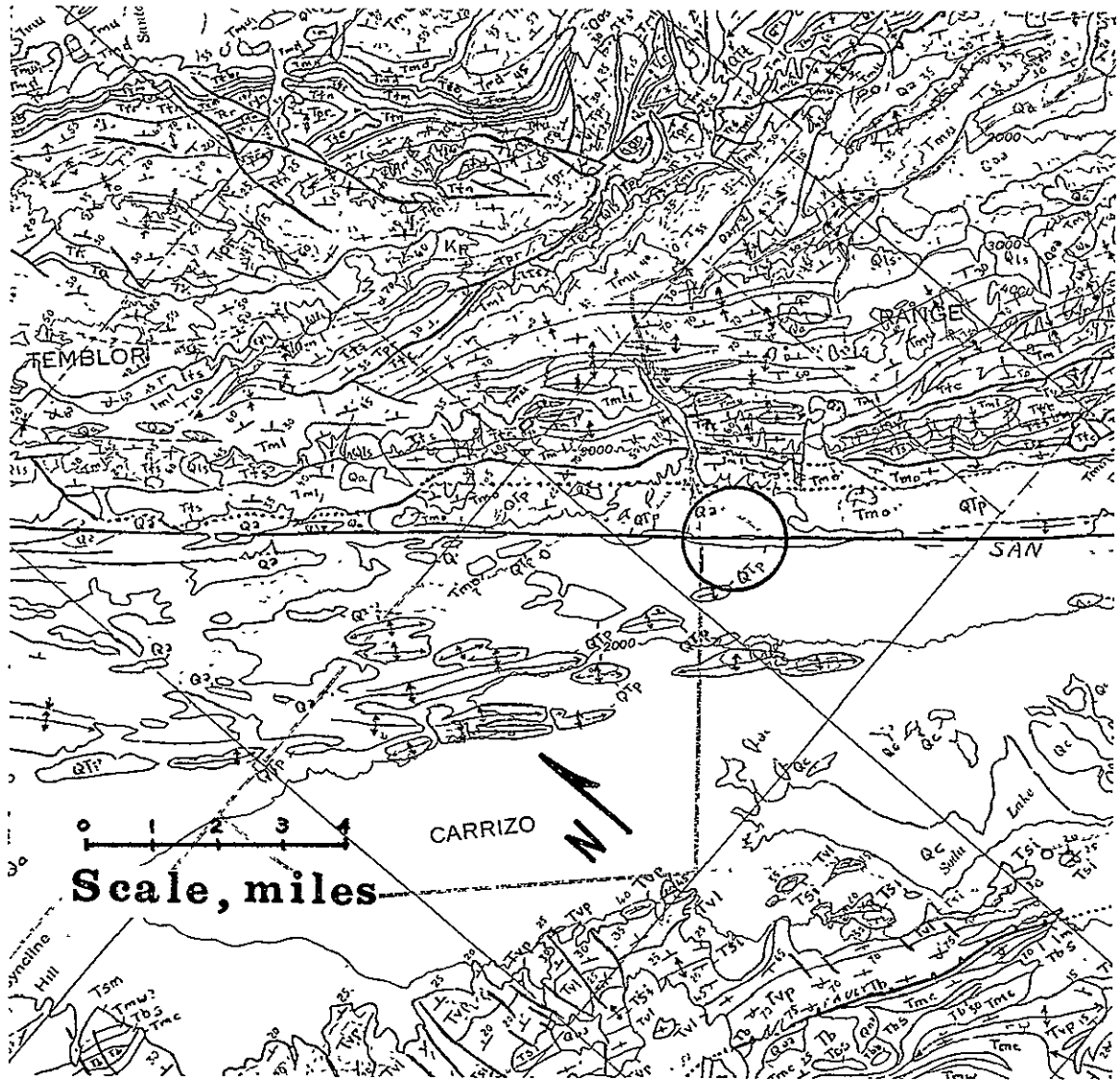
Figure 2 - Geologic map of area of study

        Qa - Quaternary alluvium
        QTp - Quaternary-Tertiary Paso Robles formation

                                  (After Dibblee, 1968)

IV. IMAGERY AND PHOTOGRAPHY

A. Infrared Imagery

The infrared image (Plate A) is a positive print of the line-scan display produced by the HRB-Singer Reconofax IV thermal infrared scanner. This image shows areal distribution of radiation intensities in the 8-13 µm, wavelength band. Areas of strong radiation (relatively higher temperature) are light in tone, while areas of weaker thermal radiation (lower temperature) are darker in tone. The intensity of the radiation emission (or radiant emittance) is a function of the 4th power of absolute temperature of the body and the emittance of the body which is, in turn, a function of wavelength.

$$\text{Radiant Emittance} = W_{8-13\mu m} = \int_{\lambda=8}^{\lambda=13} \varepsilon_\lambda \sigma T^4$$

ε_λ = spectral emittance (8-13µm bandpass)

σ = Stefan-Boltzmann constant

T = absolute (surface) temperature of the body

The non-rectilinear geometry of the images is a result of constant-angle-of-rotation in the scanning system. This fact is minimized as the area under study occupies the central linear portion of the image and it is then relatively undistorted.

The strip of image was produced from 0523 to 0535 PDT ("pre-dawn") on June 17, 1965. Pre-dawn imagery was chosen because at that time, the differential heating effect of the sun is at a minimum. The image is part of sensor data obtained in NASA926 CV-240A, Mission 10, Site 4.

PLATE   A

The specific portion of the image chosen for detailed study is part
of a much longer strip running for many tens of miles longitudinally
along the San Andreas Fault. A prominent thermal anomaly can be observed
along most of the fault zone, and in places this becomes very sharp
and narrow. In the area investigated, this anomaly corresponds di-
rectly with the topographic expression of the fault trace. The imagery
also shows temperature patterns associated with physiographic and cul-
tural features such as stream valleys, roads, cultivated fields, and
trails across section lines. Most of these features already have been
explained by Wallace and Moxham (1966).

B. USGS Aerial Photography

Stereographic inspection of the conventional high altitude aerial
photographs of the area confirmed that the localities showing the lowest
temperatures were also associated with marked breaks in slope. Field
checks confirmed this concept. The scale of these photographs, however,
is too small to allow precise differentiation of ground details that
might be used to explain the observed thermal differences. A copy of
the USGS aerial photograph of this area is included as Plate B.

PLATE   B

9
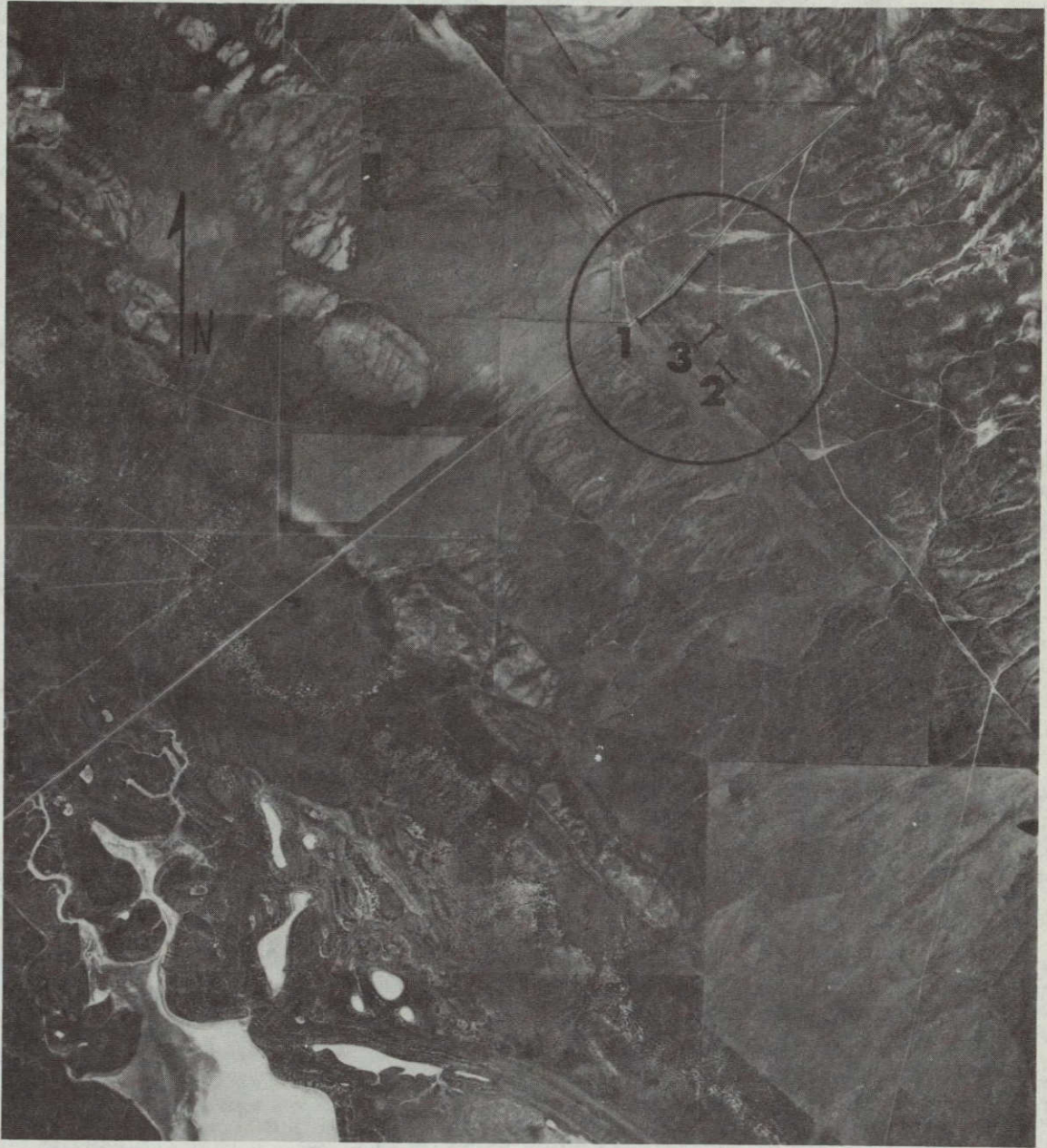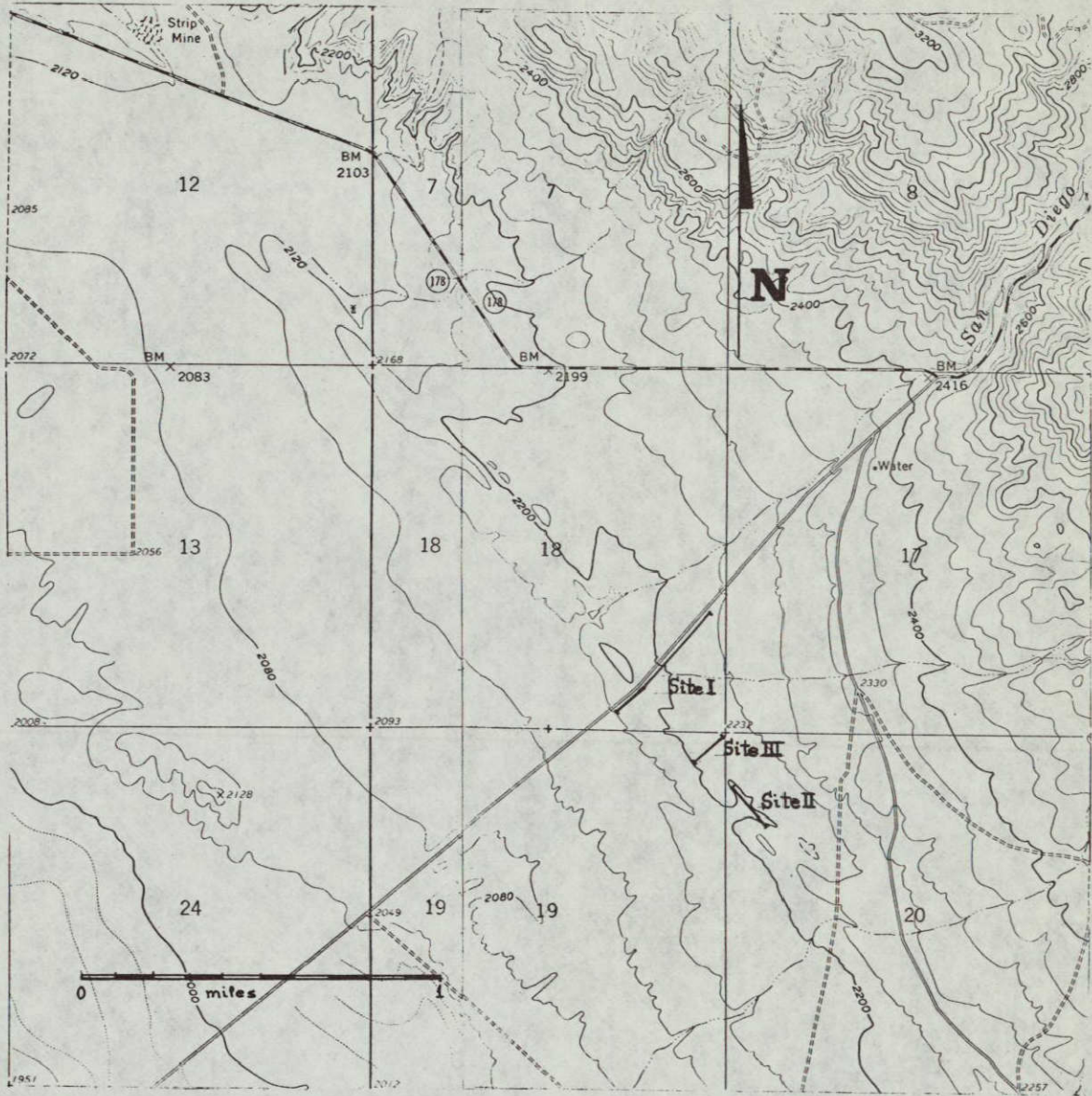
Figure 3 – Map showing location of Site #1, #2, and #3
Carrizo Plains, California

(Reproduced from Simmler and McKittrick Summit,
USGS topographic quadrangles, 7.5 minute series.)

V. LOCATION OF THE SITES FOR THE TRAVERSES

The aerial photographs and infrared images initially served as
guides for the location of the sites for the traverses. Their exact
location was determined for the following reasons: 1. No significant
lithologic change across the fault trace in the area of interest was
indicated on the geologic map (Figure 2). Thus complications of the
data due to thermal inertia and emittance differences were minimized.
2. Sites I and III showed the largest change in grey-scale contrast
across the fault trace in the thermal image. Site II includes a sharply-
defined, V-shaped thermal anomaly perpendicular to the fault trace.
3. About 200 pounds of intrumentation required roads and topographic
features which could be traversed with a vehicle. Plate B and Figure 3
show the exact location of the sites of the traverses.

VI. RADIOMETRIC EQUIPMENT

Radiometric temperatures* were measured with Barnes PRT-5 and PRT-10* non-contact, infrared radiation thermometers. The PRT-10 is still in an experimental state and it was used mainly to test its reproducibility and accuracy under field conditions. A Barnes PRT-4* radiometer was available for a back-up.

The PRT-5 consists of a 28.5 pound, portable, battery-powered unit with a 2 degree (nominal) field of view and is filtered to the 8 to 13 micron spectral region. It was capable of measuring temperatures from -20° C to +75° C. Absolute system accuracy is stated to be ±0.5 degrees Centigrade and is achieved by precisely controlling the temperature of a 45° C ± 0.5° C, in-line blackbody reference cavity within the optical head. Incoming target radiation, detected by a thermistor, is compared continuously with the known radiation from this internal reference by chopping at 90 Hertz. The difference, proportional to target temperature, is converted into an electrical signal.

The smaller PRT-10 radiation field thermometer weighs two pounds, has no moving parts and uses a vibrating tuning-fork for an optical chopper. It employs an evaporated thermopile as the infrared detector which maintains constant sensitivity, independent of ambient temperature changes. The field of view is approximately 35 degrees and the filtered bandpass is 6.9-20 microns. The temperature range is -10° C

---

*Both the PRT-10 and PRT-4 were provided by Barnes Engineering (F. Stang) for our use in this study.

to 60° C with 1° C readability. Two modes of operation are available, absolute temperature and relative temperature over a 10° C range.

Relative humidities were measured with a Bendix psychrometer model ML-450 A/UM using an air-aspirated wet and dry bulb mercury thermometer. It is battery-operated and hand-carried. Ground contact temperatures were measured using thermistor probes with a 4-channel Digitec (model 501) digital thermometer system. A simple Weston bime-tallic probe thermometer was also used. Wind velocities were measured using a hand-held Venturi-type meter. A Moseley strip-chart recorder was used in making the records of the "continuous-moving" and "sweep" traverses. Electronic equipment, not battery-operated, was powered by a Honda 300 watt motor generator.

VII. PROCEDURES

A. Stationary Measurements

PRT-5 radiometric measurements were obtained by pointing the sensor head of the radiometer vertically downward, and holding it stationary at a distance of 12 and 60 inches from the surface of the ground. Average readings were recorded. PRT-10 radiometric temperatures were obtained in the same fashion, except at a distance of 36 inches from the surface. The PRT-5 setting for the whole experiment was bandwidth 3 hertz and "medium" scale.

Contact surface temperatures were obtained with the Digitec digital thermometer by implanting the "banjo" thermistor probe at the very surface of the soil (among the roots of the vegetation), but not more than 0.25 inch into the ground. The probe was allowed to equilibrate for 60 seconds before the measurement was taken.

Contact surface temperatures at 3 inches depth were obtained with the Digitec thermometer by forcing the rod probe into the ground. In cases where the ground was very hard the soil was loosened with a geology pick, the probe quickly implanted, and the soil packed back down by hand. The probe was allowed to equilibrate for 60 seconds before the measurement was taken.

Air temperatures were recorded by means of thermistor probes and the Digitec thermometer. The probes were attached to the bumper and top of the truck at heights of approximately 12 and 84 inches above the surface of the ground. Air temperatures were recorded nearly simultaneously with the ground temperatures.

Procedures followed in obtaining relative humidity and wind velocity are routine. "Sky temperature" was obtained by pointing the PRT-5 vertically upward. Sky conditions (i.e. clouds) were recorded from visual inspection. During these nights there was a full moon.

B. Mobile Measurements

Two types of mobile measurements were made, both from the truck. A "sweep" traverse and a "continuous moving" traverse. For the "sweep" traverse the terrain-target around the stations, about 12 to 15 feet from the optical head, was swept with the PRT-5 with a sweeping radius of about 10 feet. These measurements were made at each station. Recording of the data was made on the strip chart recorder to obtain a mean and an assessment of the variances of the temperature at each station. Also air temperatures were taken concurrently at heights of 12 and 84 inches.

The "continuous moving" traverse consisted of a continuous temperature profile of the terrain along the station-line. This was achieved also with the PRT-5 by pointing the optical head towards the target with a 30° angle of inclination and from a height of three feet. The data for this traverse was taken with the recording system in continuous operation and with a truck ground speed of 5 mph.

VIII. FIELD WORK

A preliminary reconnaissance was made on the afternoon of May 31, 1969. This most important step consisted of determination of the position of the station lines in the field and measuring the locations of each station in advance of the nighttime measurement. The stations were located with steel tape and marked with wooden stakes and red reflector tape. Photographs were taken of the area of each of the station lines with a 35 mm camera using Agfachrome color film, ASA 50, at 1/250 sec., and f11.

A. Site I

The traverses at this site paralleled the major asphalt road shown on the map and included one stationary traverse, one sweep traverse, and one continuously moving traverse of both sides of the road. Measurements were taken on June 1, 1969 at 41 stations placed 50 feet apart. This station line extended approximately 1000 feet to either side of the falt zone and crossed it approximately perpendicularly. All measurements for the stationary and sweep traverses were made on the SE side of the road about 10 feet from the road and the continuously moving traverses were made on both sides of the road. (Figures 4, 5, 6, and 7)

Table 1 gives the calibration data taken from Site I for the PRT-5 using 15° conical blackbody surrounded with a water jacket. Table II gives the calibration data at Site I for the thermistor probes and the Digitec digital thermometer with the probes immersed in a pan of water. The difference in calibration of the PRT-5 at 0105 hrs. versus 0350 hrs.

16
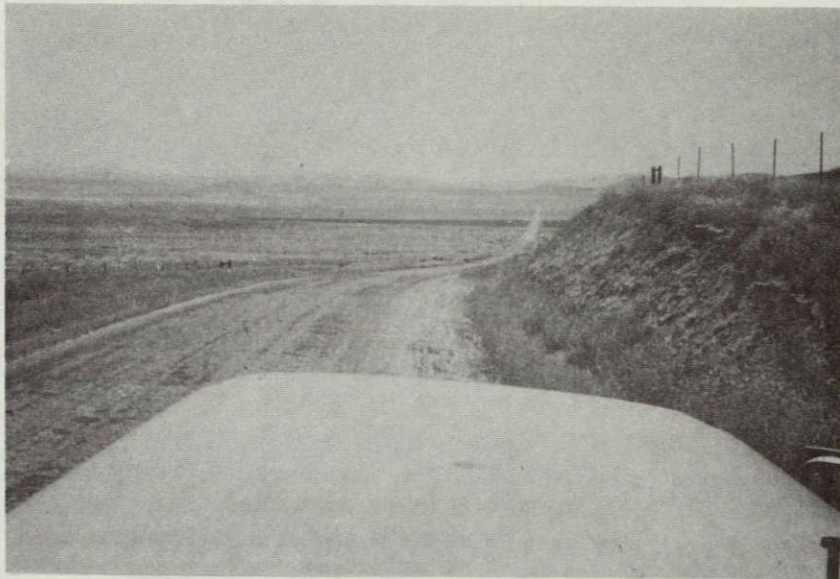
Figure 4 - Photograph taken at station I-23, looking SW of Site I. All traverses were made on the left side of the road, except for one continuously moving traverse on the right side of it. Station I-23 is located close to the intersection of the Station line and the San Andreas Fault trace. The Paso Robles Formation is shown on the road cut at right.
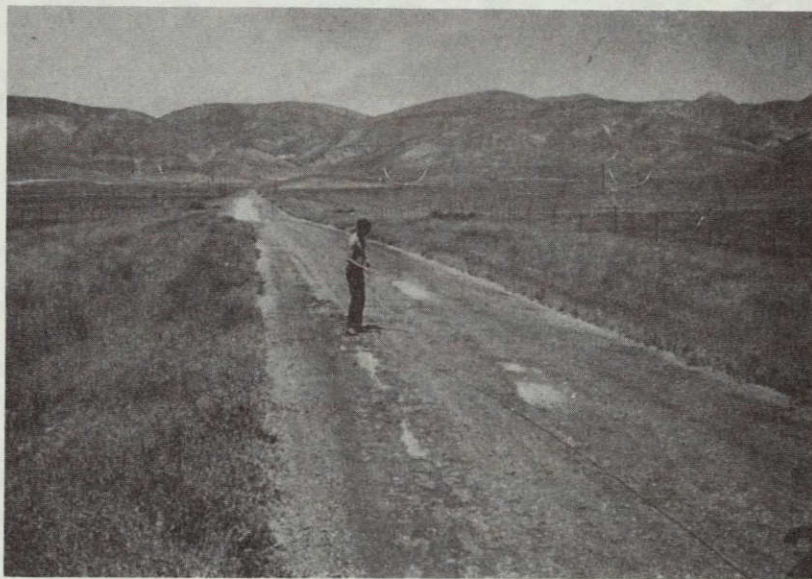
Figure 5 - Photograph from station I-23, looking NE, of site.
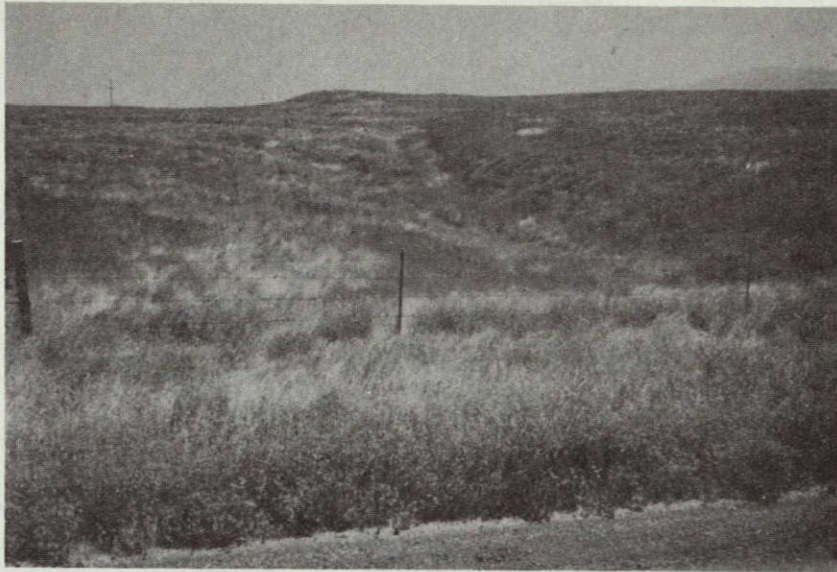
Figure 6 - Photograph at station I-23, looking SE along the
trace of the San Andreas Fault. Note the change
in vegetation density across the fault.
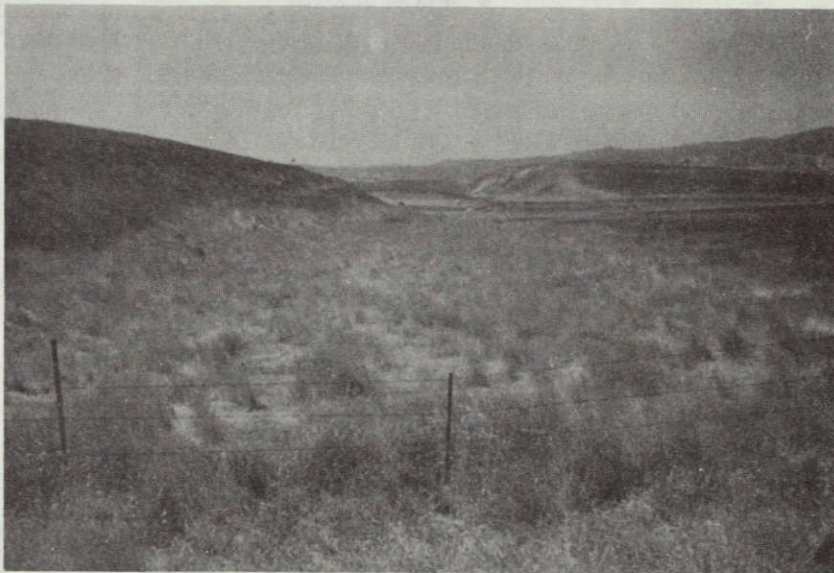
Figure 7 - Photograph from station I-23 looking NW along the
San Andreas Fault trace. Note change in vegeta-
tion density across the fault trace.

is unexplainable except as a long-time drift. The calibration data for the thermistor probes indicates they are well within the limits required for our study. Since calibration errors were small, no calibration corrections have been made in the data presented in this report. The stationary traverse started at station 1-41 at 0105 PDT and proceeded NE to station 1-1 at 0350 PDT. The sweep traverse started at 1-41 and proceeded NE to station 1-1.

Table I. Calibration of PRT-5 for Site I

Station 1-41   Time 0105 PDT

Station	Time (PDT)	Radiometric temperature of conical blackbody	Contact temperature of Conical Blackbody (with Mercury Thermometer)
1-41	0105	22.1° C	22.0° C
1-1	0350	19.5° C	18.5° C

Table II. Calibration of Digitec for Site I

Four repeated readings (°C) were taken.

Thermistor # 1	20.71	20.82	20.89	20.81
Thermistor # 2	20.35	20.43	20.51	20.43
Thermistor # 3	20.75	20.82	20.95	20.84
Thermistor # 4	20.80	20.93	20.97	20.90
Mercury Therm.	21.00	21.00	21.00	21.00
Weston Probe	20.00	20.50	20.30	20.30

Thermistor #1 was used to measure the contact temperature of the soil surface, thermistor #2 to measure the contact temperature of the

soil at a depth of 3 inches, thermistor #3 to measure the air temperature 84 inches above the ground and thermistor #4 to measure the air temperature 12 inches above the ground.

Soil samples were taken concurrently at the same sites as the temperature measurements. About 60 to 80 grams of surface soil were collected in air-tight glass sample bottles.

B. Site II

The traverse at Site II was stationary and approximately parallels the San Andreas Fault, crossing the prominent V-shaped anomaly previously noted on the infrared imagery. The station line originally consisted of 70 stations spaced at 10-foot intervals crossing two stream valleys and an intervening hill. (Figures 8, 9, 10 and 11) Measurements, however, were not taken at all stations except in the two valleys which gave the strongest anomalies on the imagery. Outside of the valleys measurements were taken at every fifth station giving a total of 32 measured stations. Relief within the area was estimated at 30 feet. All equipment for Site II was carried by hand and equipment requiring 110-volt power sources were omitted. Sampling started at NW end of the station line at station 2-1 and proceeded SE to station 2-70. Equipment calibration given in Table III was the same as for Site III.

C. Site III

The station line for Site III crosses the San Andreas Fault perpendicularly and consists of 12 stations at 50-foot intervals. The

20
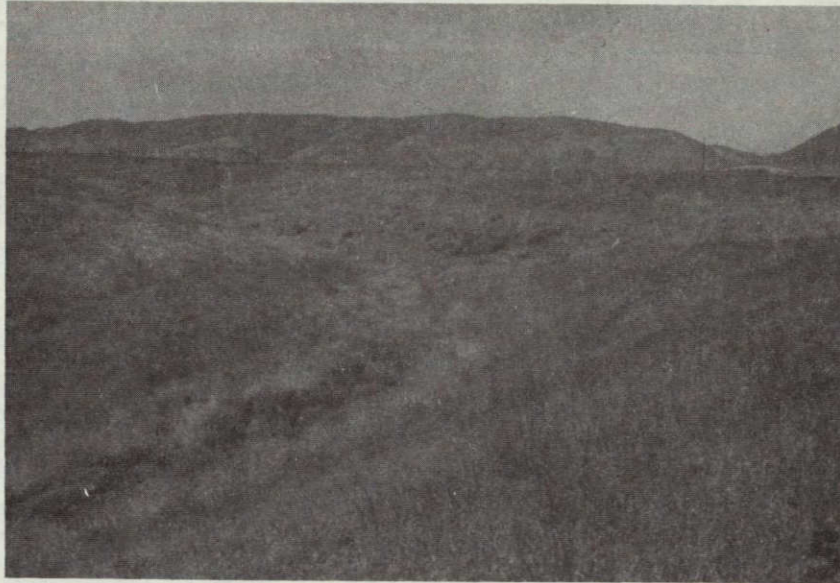
Figure 8 – Photograph taken from the small hill in the middle
of Site II looking NE along the station-line and
approximately parallel to the fault trace. From
lower left to the central part of the picture is
the small valley which showed such a strong thermal
anomaly. Again, note the change in vegetation as one
nears the bottom of the valley. The bottom of the
gully was filled with about three feet of dried
tumbleweed.
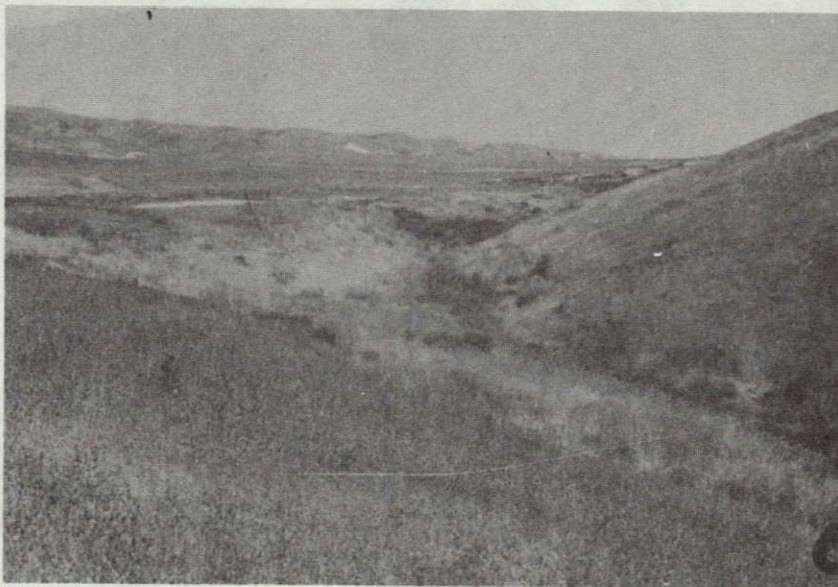
Figure 9 – Photograph taken from the same locality as
Figure 8 looking SE along the other valley
of the V-shaped thermal anomaly. Again note
the change in vegetation and tumbleweed
accumulations.

21
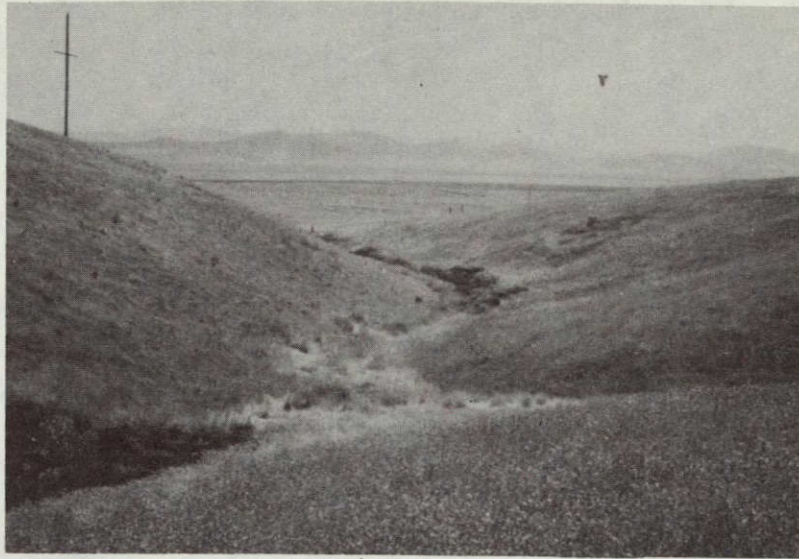
Figure 10 - Photograph taken from the same station as
Figure 9 looking SW down the confluence of
the two small valleys.

Figure 11 - Close-up of the bottom of the gully shown
in Figure 8. Note the vegetation change
and accumulation of tumbleweed.

line extends approximately 200 feet SW of the fault trace and approximately 400 feet NE of the trace. Sampling was started at station 3-1 at 0100 PDT June 2, 1969 and proceeded to station 3-13 ending at 0150 PDT. Calibration of the PRT-5, made at 0045 PDT and used for Sites II and III, is given in Table III. All equipment for Site III was truck-mounted. A continuously moving traverse was also made at this site. Again, the data here was not corrected for calibrations.

Table III. Calibration of PRT-5 for Sites II & III

Radiometric temperature of conical blackbody	Contact temperature of conical blackbody with mercury thermometer
21.1° C	22.0° C

IX. SOIL MOISTURE EXPERIMENT

A. Experimental Procedure

To examine one of the many variables involved, the effect of soil moisture on radiometric temperature was investigated. At approximately 0030 PDT, June 1, 1969, near station 1-23 of Site I, four 10" × 12" × 3" aluminum foil baking pans were set on the ground. The first pan contained 1.5 inches of surface soil with no added water, the second pan contained 1.5 inches of surface soil with 7 fluid ounces of added water, the third pan contained 1.5 inches of surface soil with 14 fluid ounces of added water, and the fourth pan contained no soil but only 32 fluid ounces of fresh water. These were allowed to equilibrate with the ground air temperatures until 0545 PDT at which time the following measurements were made:

1. Radiometric temperature (PRT-5) 12 inches from the surface of the pan.

2. Contact temperature with thermistor and Digitec, one inch below the surface, allowing 60 seconds for the probe to equilibrate.

3. A soil sample for future moisture-content measurements.

B. Moisture Content Analysis

The soil samples collected from Site I stations and experiment pans were processed as follows:

1. The caps were removed from the air-tight sample bottles and the bottles were weighed on a 200 gm.-capacity Mettler Micro-balance with a balance precision of ±0.0002 grams.

2. The bottles and contents were heated in a vacuum oven at 110° C for 16 hours.

3. The bottles and contents were cooled and re-weighed.

4. The weight percent of moisture* and volatiles was calculated.

C. Results of Soil Moisture Experiment

The following Table IV gives the temperature and percent moisture obtained at approximately 0545 PDT on June 1, 1969, from the four pans of soil and water. Figure 12 presents the same data in graphical form. Relative humidity was approximately 60 percent and air temperature at 12 inches from the ground was approximately 14° C.

---

*There was some concern as to whether this heating was in fact driving out some of the inter-layer water of the clay structures. This effect should be minimal. Deer, Howie, & Zussman (1962) state that the inter-layer water (OH) of the montmorillonite clays is lost at temperatures between 100 and 250° C. Some water (OH) remains, only to be lost at temperatures of 300° C. Inspection of d.t.a. curves for many montmorillonite-type clay minerals show that most of the (OH) water is lost at temperatures well over the 110° C used in our heating. Most water is lost at temperatures ranging from 150 to 200° C. D.t.a curves for illites show that most inter-layer water (OH) is lost at temperatures of 100 to 200° C and in kaolinites some adsorbed and inter-layer water lost upon heating to 110° C with most of the water (OH) coming off gradually up to 400° C.

Thus, although some of the water driven off in the heating up to 110° C may have been inter-layer water of the clays, it is safe to assume that the greater percentage was indeed interstitial or pore water.
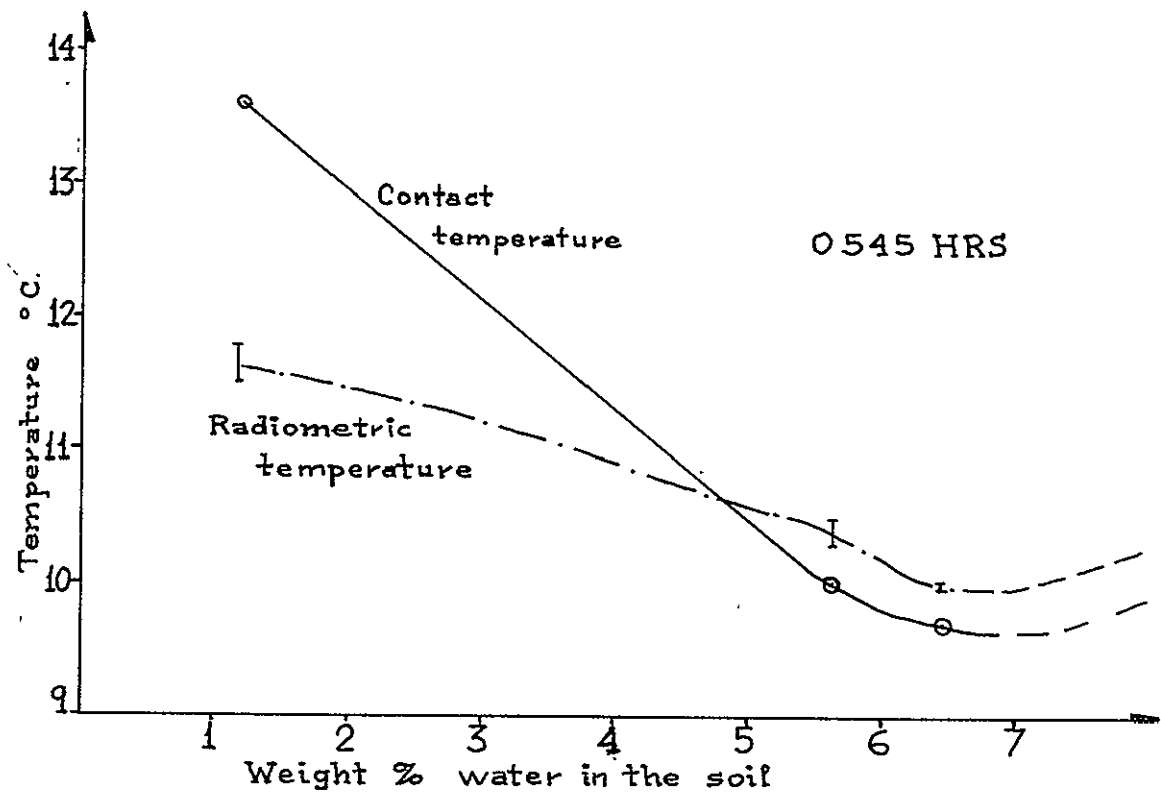
Figure 12 – Data from Table IV shows the relation between
contact and radiometric temperatures as a
function of the moisture content of the soil.

Table IV. Soil Moisture Data at 0545 hrs.

	EXP-1	EXP-2	EXP-3	EXP-4
Radiometric temperature PRT-5, 12 inches from surface	11.5 11.8	10.3 10.5	10.0 10.0	12.0 12.0
Average of radiometric temps.	11.6	10.4	10.0	12.0
Contact temperature with thermistor probe (-1")	13.6	10.0	9.7	11.0
Moisture content (weight %)	1.20	5.63	6.46	*****

Air temperature, 14° C and relative humidty, 60%
EXP-1 is for dry soil (natural state)
EXP-2 is soil plus 7 fluid oz. of water
EXP-3 is soil plus 14 fluid oz. of water
EXP-4 is 32 fluid oz. of water only

The following conclusions can be drawn from the soil moisture and temperature data. First, the cooling of the soil appears to be a function of the moisture content; the soil containing more water showed greater cooling, at least up to 6.5% moisture content. This cooling phenomena was detected both by the radiation thermometer and the contact thermistor probe. Second, this change in temperature of the soil with water content suggests that active evaporation of the water in the soil was taken place at the surface. Third, the radiometric temperature of the water was higher than that of any soil-water mixture. However, the water had cooled from its original temperature (of about 20° C) to a value lower than either air temperature or "dry" contact soil temperature, indicating that indeed evaporative cooling was taking place.

Fourth, the radiometric temperatures of the soil are lower than contact temperatures one inch below the surface for the two lower moisture-content soils. This relationship is inverted for higher moisture content soils, however, and seems to take place at about 5% ·moisture content.

X. RESULTS

A FORTRAN IV program was written to compile and plot all of the digital data collected. A description of the program is given in Appendix I. The rough data was smoothed using a simple nine-point running average-type smoothing formula. Overlays of the graphs combining several of the variables have also been produced.

For all three sites, the skies were clear and sky temperature was less than -20° C, the lowest limit of temperature sensitivity of the PRT-5. A full moon prevailed during both nights. Wind velocity varied from zero to six miles per hour and we can show no direct effect of the wind velocity on any of the measurements.

A. Site I

Upon inspection of Figures 13 and 14, the following facts are evident:

1. On the average, the highest temperatures measured at night were the contact temperatures at 3 inches depth. The lowest temperatures measured were those taken with the PRT-5. All three types of PRT-5 measurements tended to cluster around the same values over most of the station line. The PRT-5 "sweep" traverse-temperatures were slightly lower than the other PRT-5 measurements because this traverse was done later in the morning (0430 PDT).

2. There exists a definite temperature anomaly across the San Andreas Fault trace at this site. This cold anomaly amounts to a 3 to 10° C differential, depending on the method used; the warmer temperatures are

29

San Andreas
Fault trace
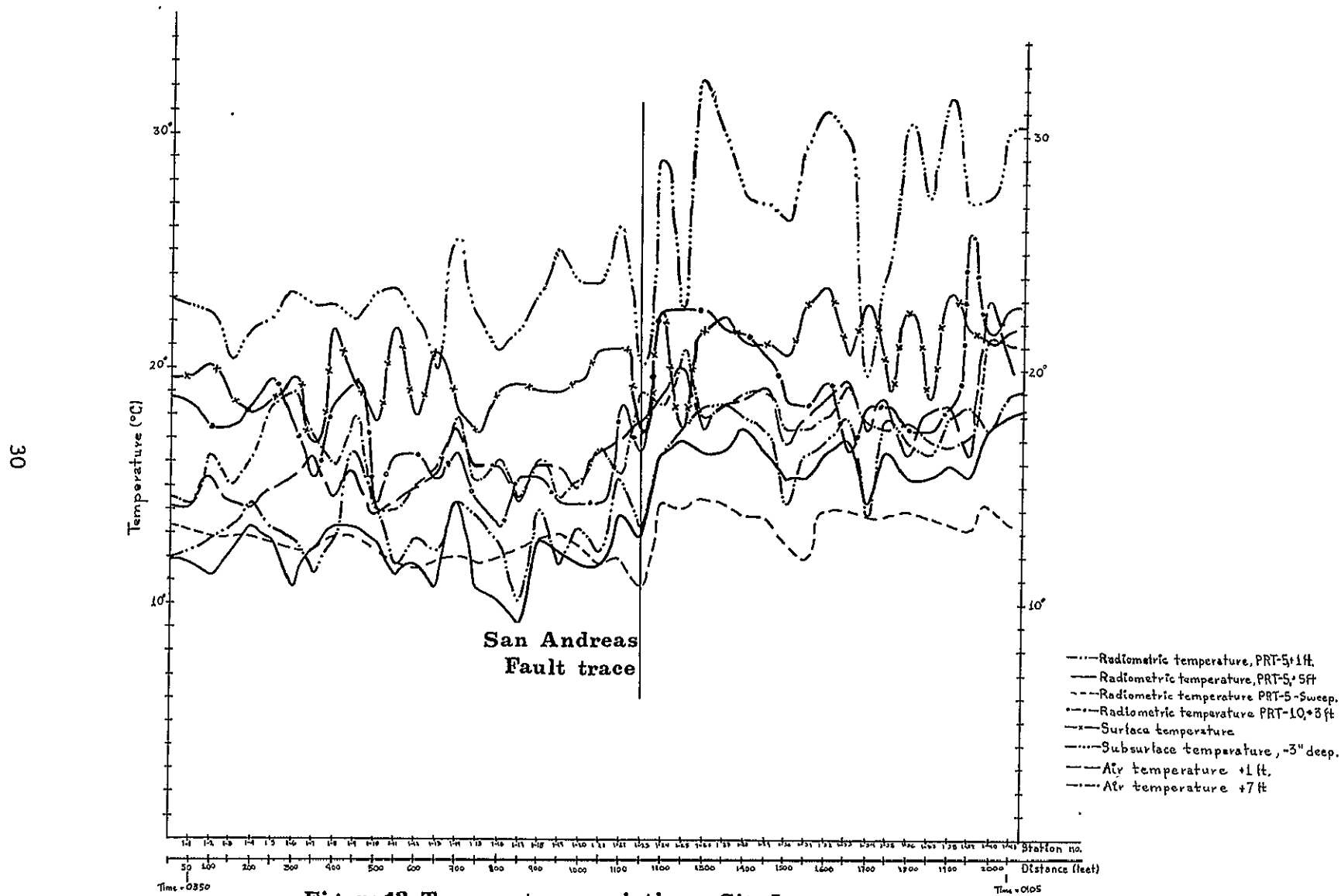
Figure 13. Temperature variations. Site I

30

San Andreas
Fault trace

——··— Radiometric temperature PRT-5 +1 ft.
——— Radiometric temperature PRT-5 +5 ft
o——o Radiometric temperature PRT-10 +3 ft.
————— Radiometric temperature PRT-5 sweep.
——•— Surface temperature
————— Subsurface temperature -3" deep.
——— Air temperature +1 ft.
——··— Air temperature +7 ft.

Time = 0350 **Figure 14. Temperature variations, smoothed curves, Site I** Time = 0105

31
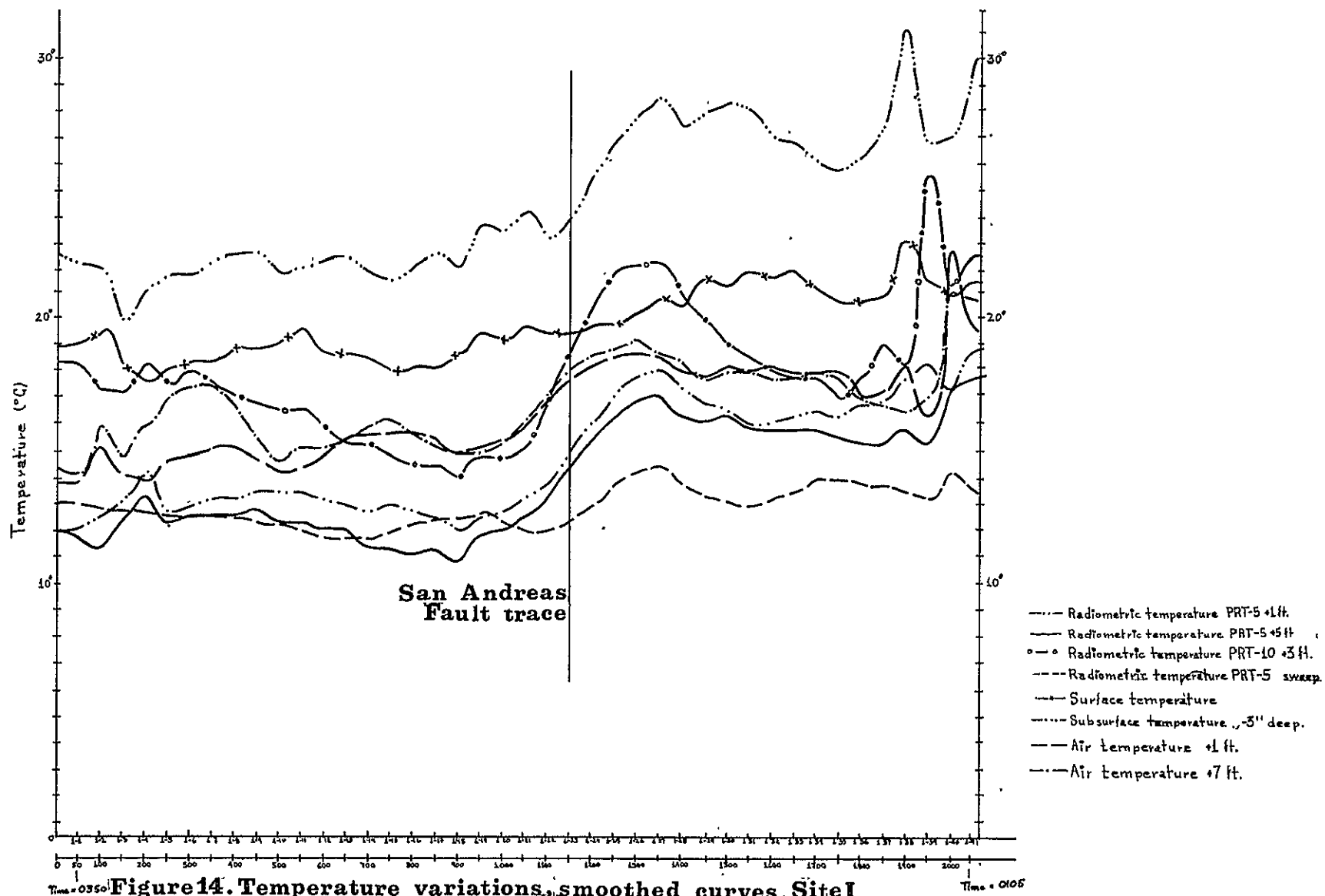
found on the SW side of the fault. This differential is especially noticeable on the smoothed graphs, but it is also detected in the rough data. Radiometric temperatures, with the exception of those from the sweep traverse, and subsurface contact temperatures show the strongest differential.

3. There is a high correlation between most of the set of temperature measurements, even at individual stations (see graphs).

Inspection of Figures 15 and 16 suggests the following relationships:

1. The moisture content of the soil as determined by the previously described method, ranges from almost 0% to approximately 3% by weight.

2. The variation of moisture content along the station line is very noticeable in the graphical data.

3. There exists an anomaly in the moisture content across the fault trace – the average moisture content on the SW side of the fault is about 1% while the moisture content on the NE side of the fault is about 1.8%.

4. There exists a strong negative correlation between soil moisture content and temperature of the soil. This is noted on both the rough and "smoothed" graphs, although the rough data shows the correlation in much more detail.

Inspection of Figure 17 comparing the PRT-5 measurements with PRT-10 measurements suggests the following:

1. The PRT-10 consistently gave higher temperature measurements than did the PRT-5 – the difference averaging about 3° C.
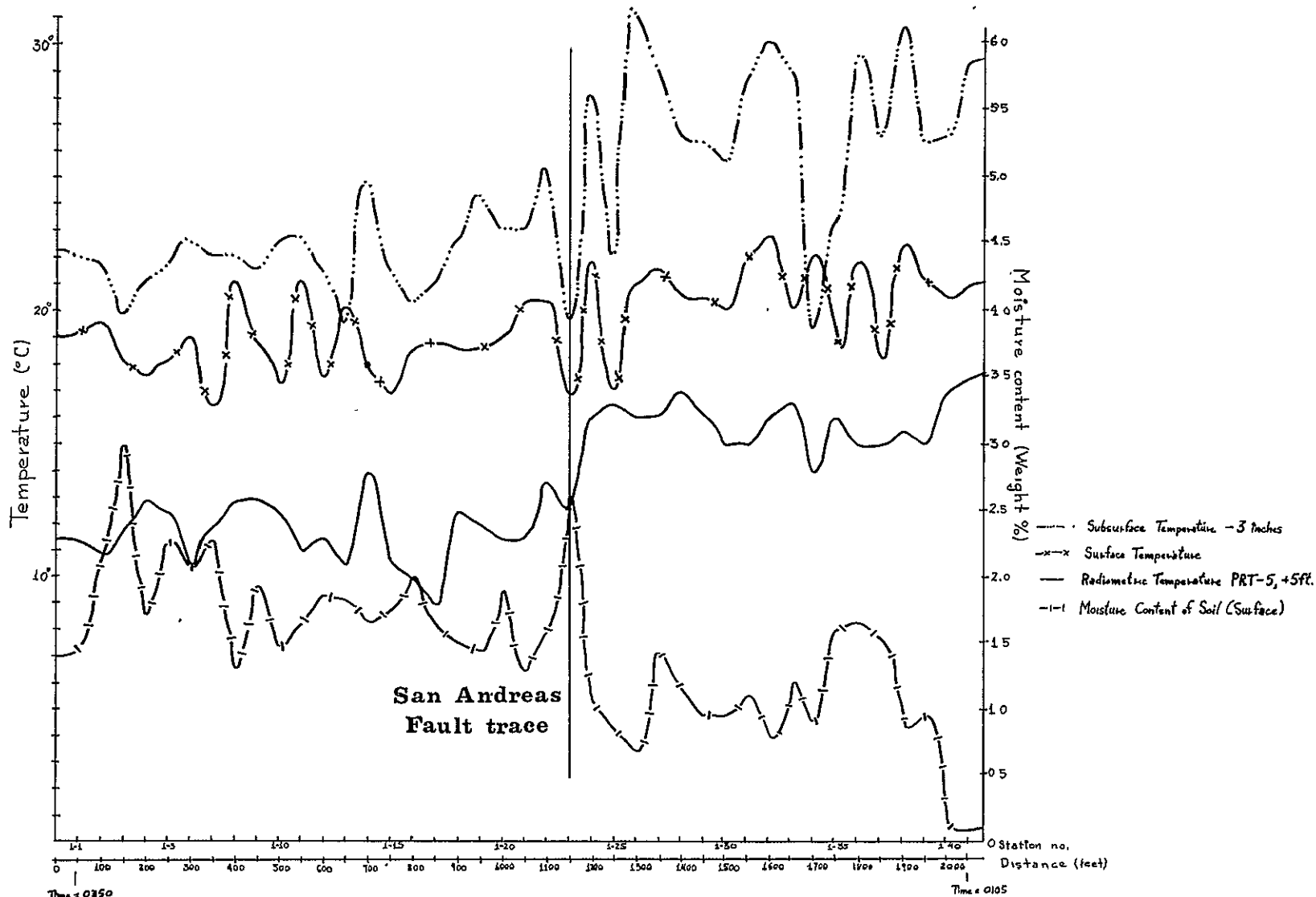
Figure 15. Temperature vs moisture content, Site I

San Andreas
Fault trace

Subsurface Temperature −3 inches
Surface Temperature
Radiometric Temperature PRT−5, +5ft.
Moisture Content of Soil (Surface)

33
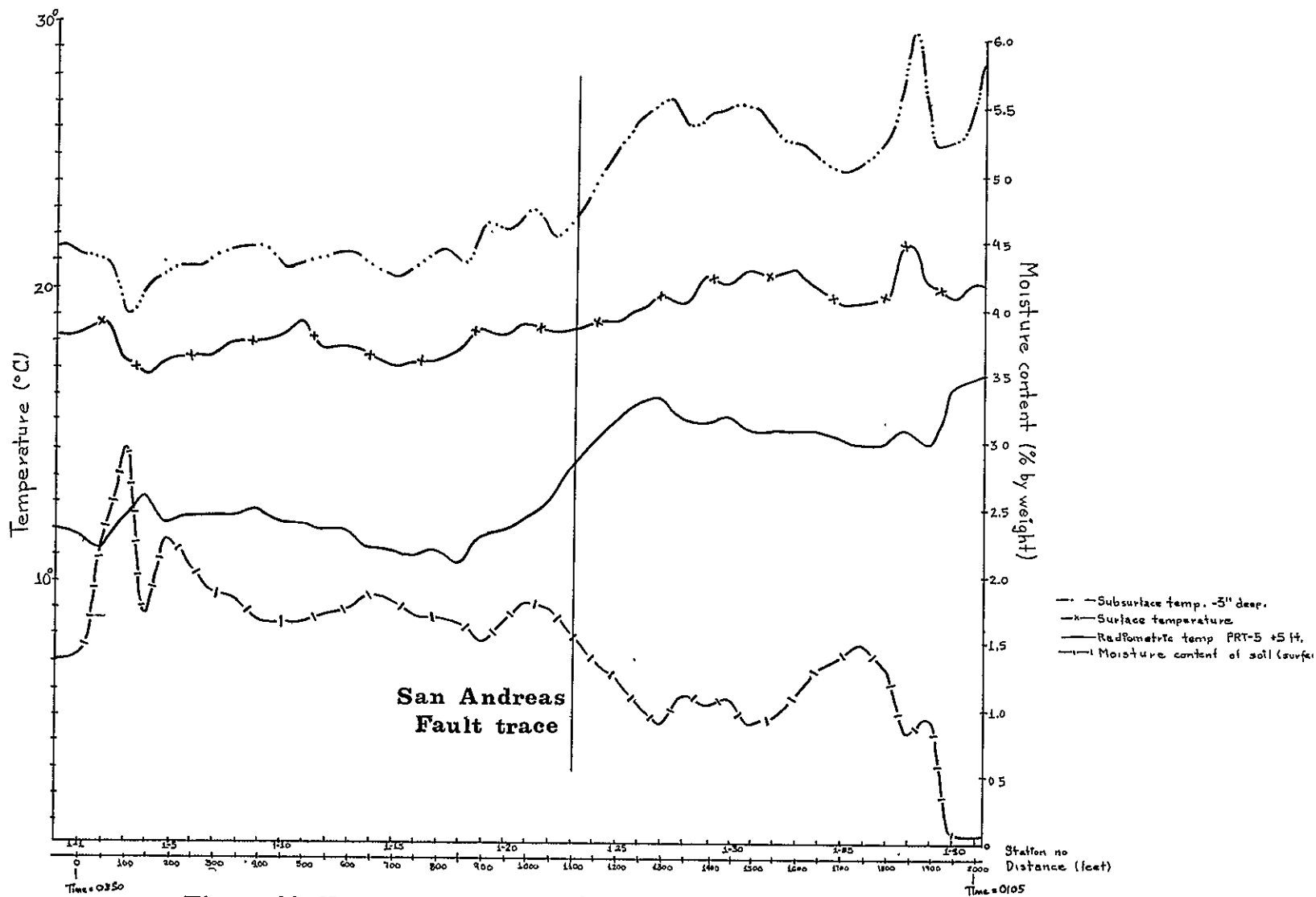
Figure 16. Temperatures vs moisture content, smoothed curves, Site I

34
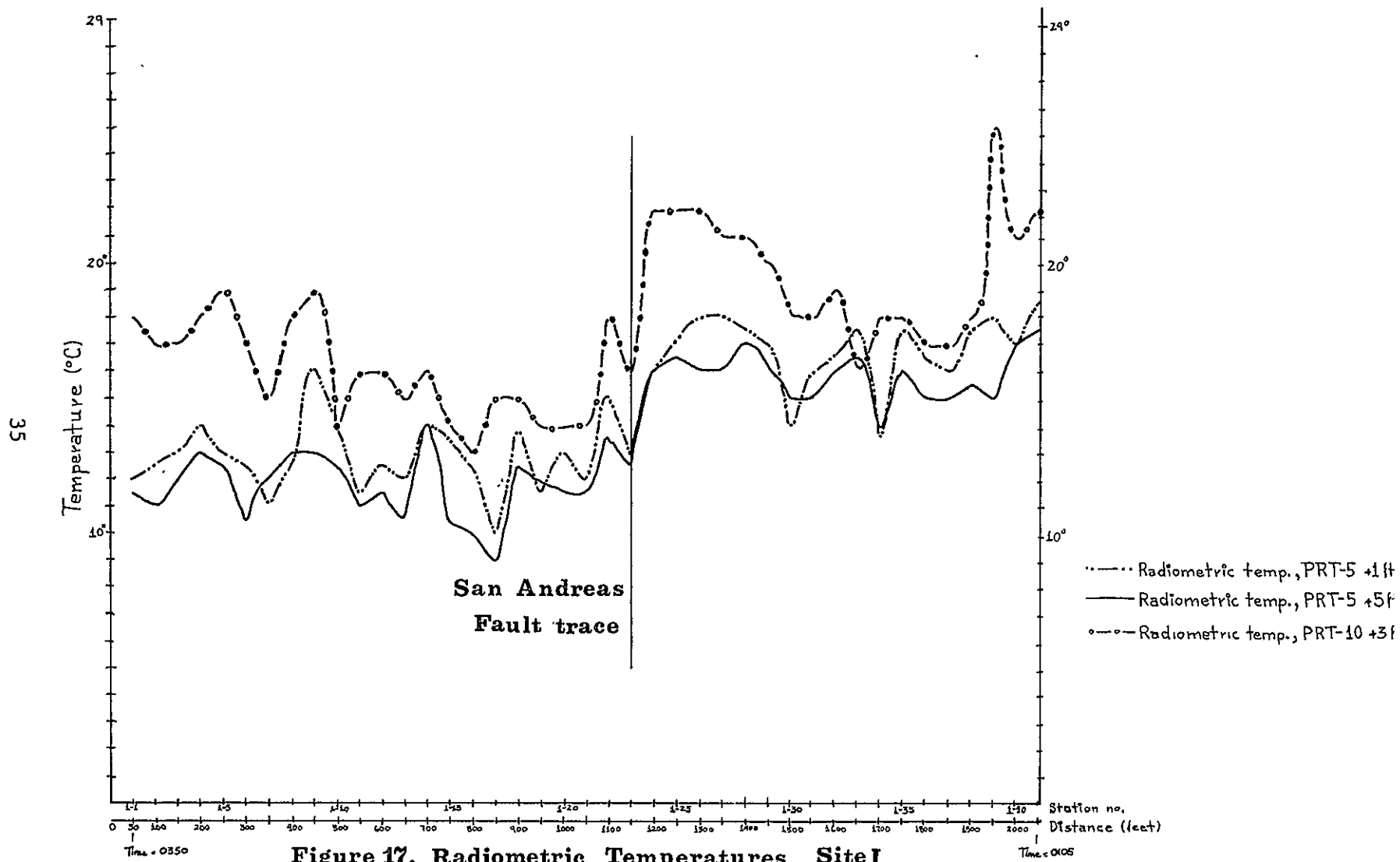
Figure 17. Radiometric Temperatures   Site I

2.   Temperature measurements taken with the PRT-5 at 12 inches above the ground surface are on the average about 1° C higher than those taken with the PRT-5 at 60 inches above the ground surface.

B.   Site II

The station line at Site II is <u>parallel to the fault trace</u> and upon inspection of Figure 18 several facts are evident:
1.   There exists definite temperature anomalies in the area of the two gullies.   These anomalies have magnitudes of 5° to 10° C, depending on the measurement-method cited.   Subsurface measurements show cold anomalies of about 10° C in both of the gullies relative to the intervening hill.   Radiometric temperatures show negative anomalies of about 6° C in the gully at station 2-28 and of about 10° C in the gully at station 2-43.   Air temperatures at 36 inches height show almost no anomaly at station 2-28 and a 5° C negative anomaly at station 2-43.   There is a high correlation among most of the temperature-measurement methods for a particular station.   On the average, the temperatures measured in the gully at station 2-28 are higher than those measured in the gully at station 2-43 (combining all methods) by about 3° C.   Radiometric measurements with the PRT-5 show <u>no consistent difference</u> whether taken at 12 inches above the ground surface or at 60 inches above the ground surface, unlike the data from Site I.

Figure 19, which includes the relative humidity measurements, shows anomalies in the relative humidity occurring in both gullies. Near the gully at station 2-28, a negative anomaly of about 14% occurs while around the gully at station 2-43 a positive anomaly of 12% occurs.
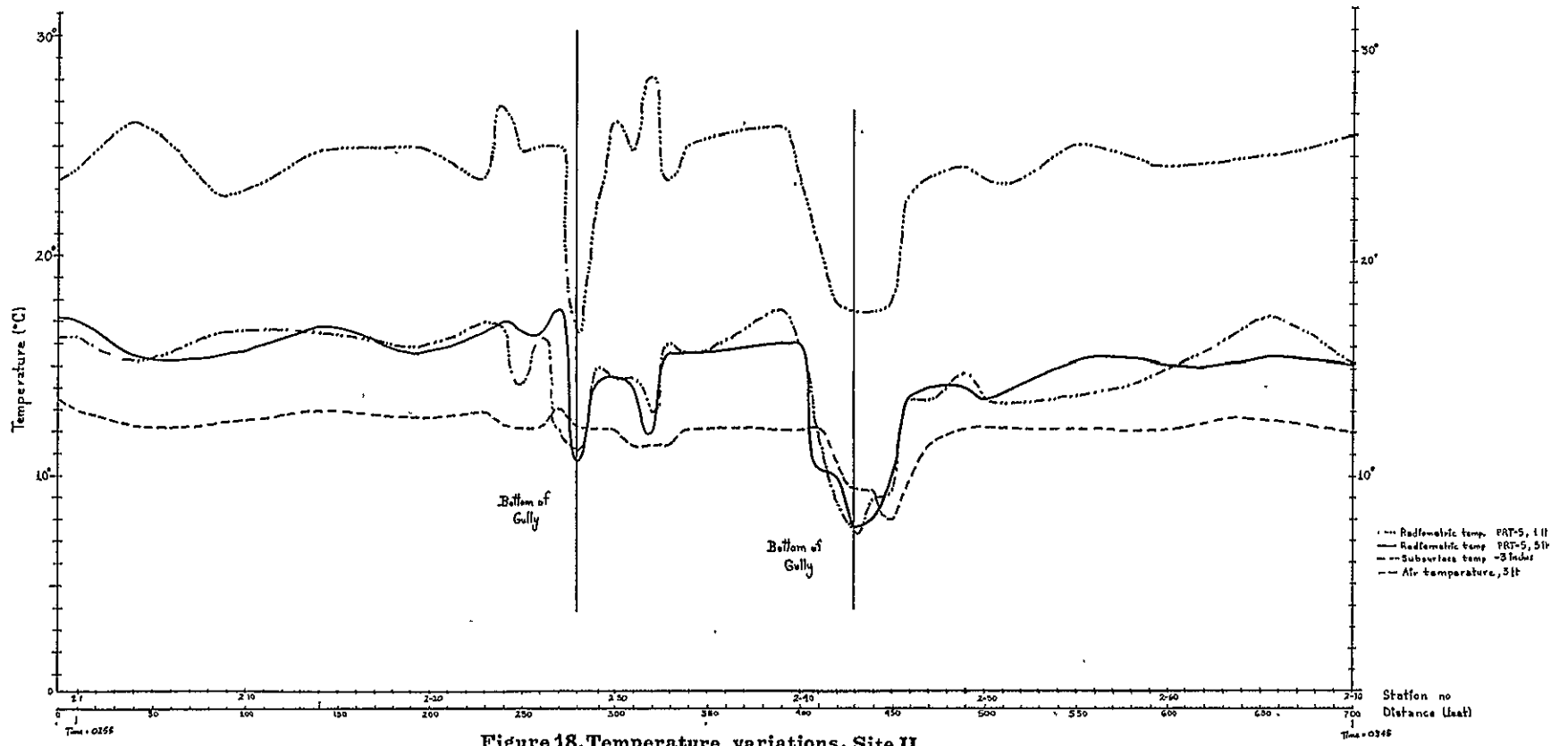
Figure 18. Temperature variations, Site II

37
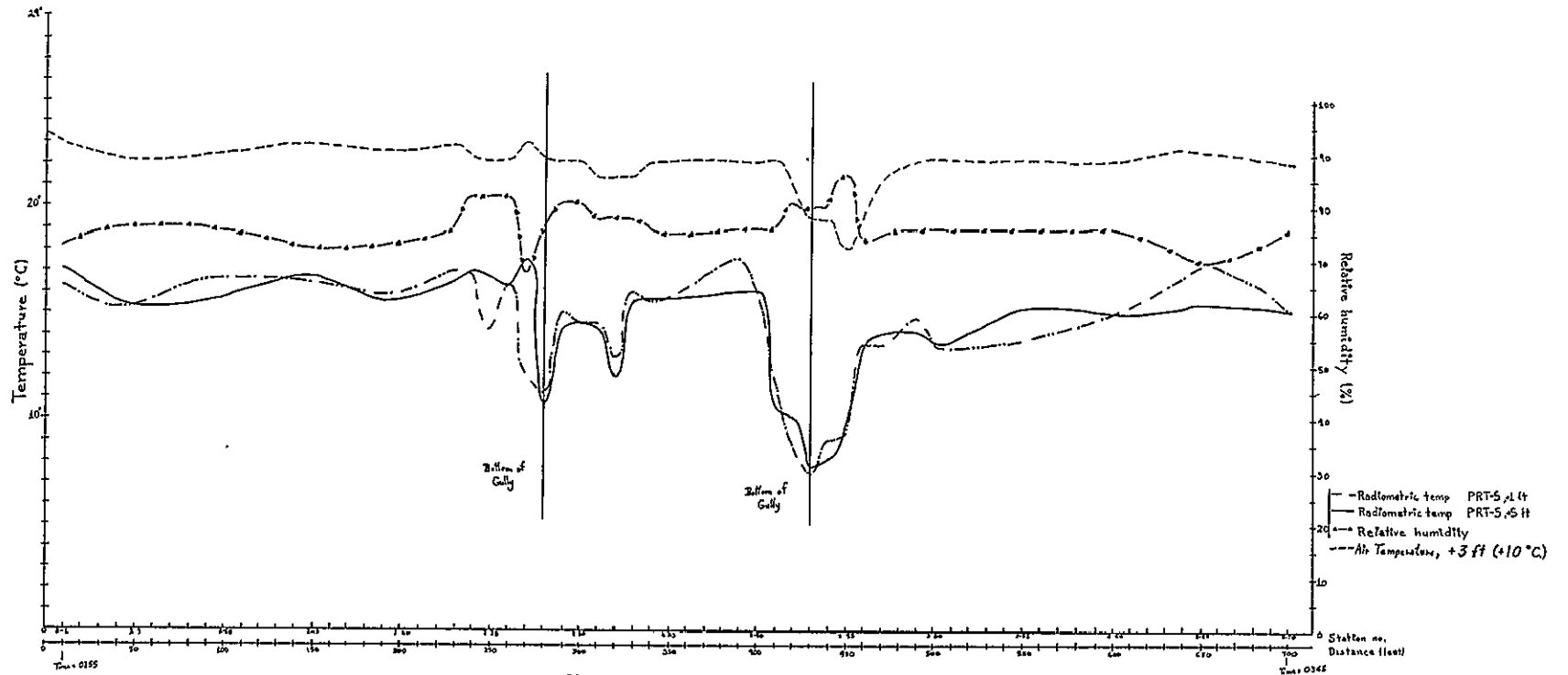
Figure 19. Radiometric Temperatures vs Relative humidity, Site II

As should be expected, there exists a strong negative correlation be-
tween air temperatures and percent relative humidity. A negative cor-
relation of less magnitude also exists between relative humidity and
radiometric temperatures of the ground.

However, it may be noted that the subsurface temperature at
-3 inches averages 6° to 7° C higher than the radiometric temperatures
at this site. While the low anomalies in the gullies for subsurface
temperatures suggests evaporative cooling is taking place, the 6° to
7° C differential suggests that the soil has a very low thermal con-
ductivity. The tumbleweed was proven to have no effect on the radio-
metric temperature - the radiometric temperature of a particular spot
with and with tumbleweed removed was the same.

C. Site III

Upon inspection of Figures 20 and 21, the following facts are
evident:

1. Of the temperatures measured by the different methods, the radio-
metric temperatures are the lowest.

2. There exists a strong anomaly across the San Andreas Fault at this
site. The magnitude of this anomaly is 3° to 18° C, depending on the
measurement-method used. The subsurface temperature is the most sensi-
tive, giving an 18° C negative anomaly while the air temperature at
84 inches above the ground surface is the least sensitive, giving a
negative anomaly of only 3° C. Most of these negative anomalies are
centered about 50 feet NE of the topographic expression of the fault.
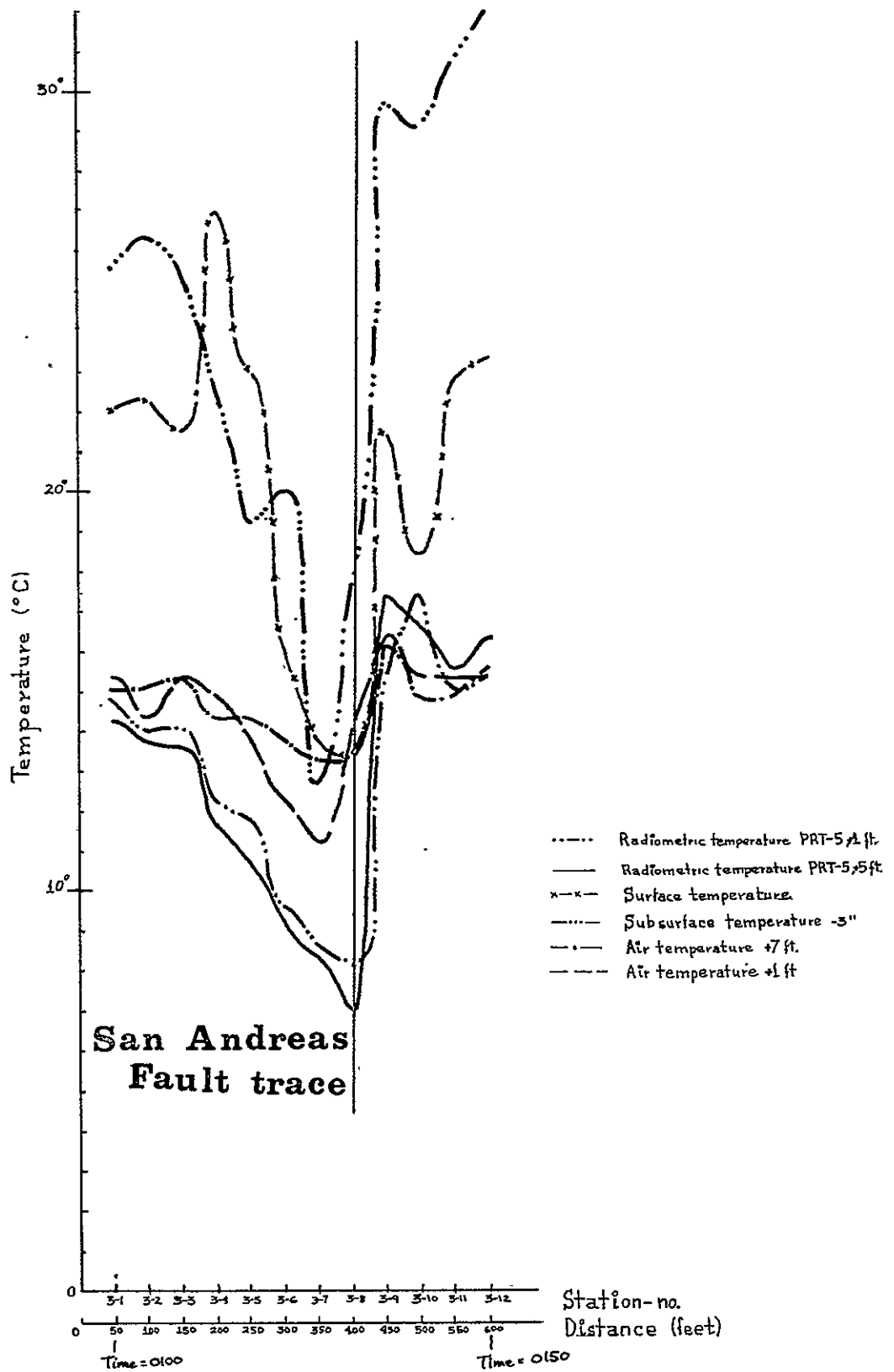
Figure 20. Temperature variations, Site I I I
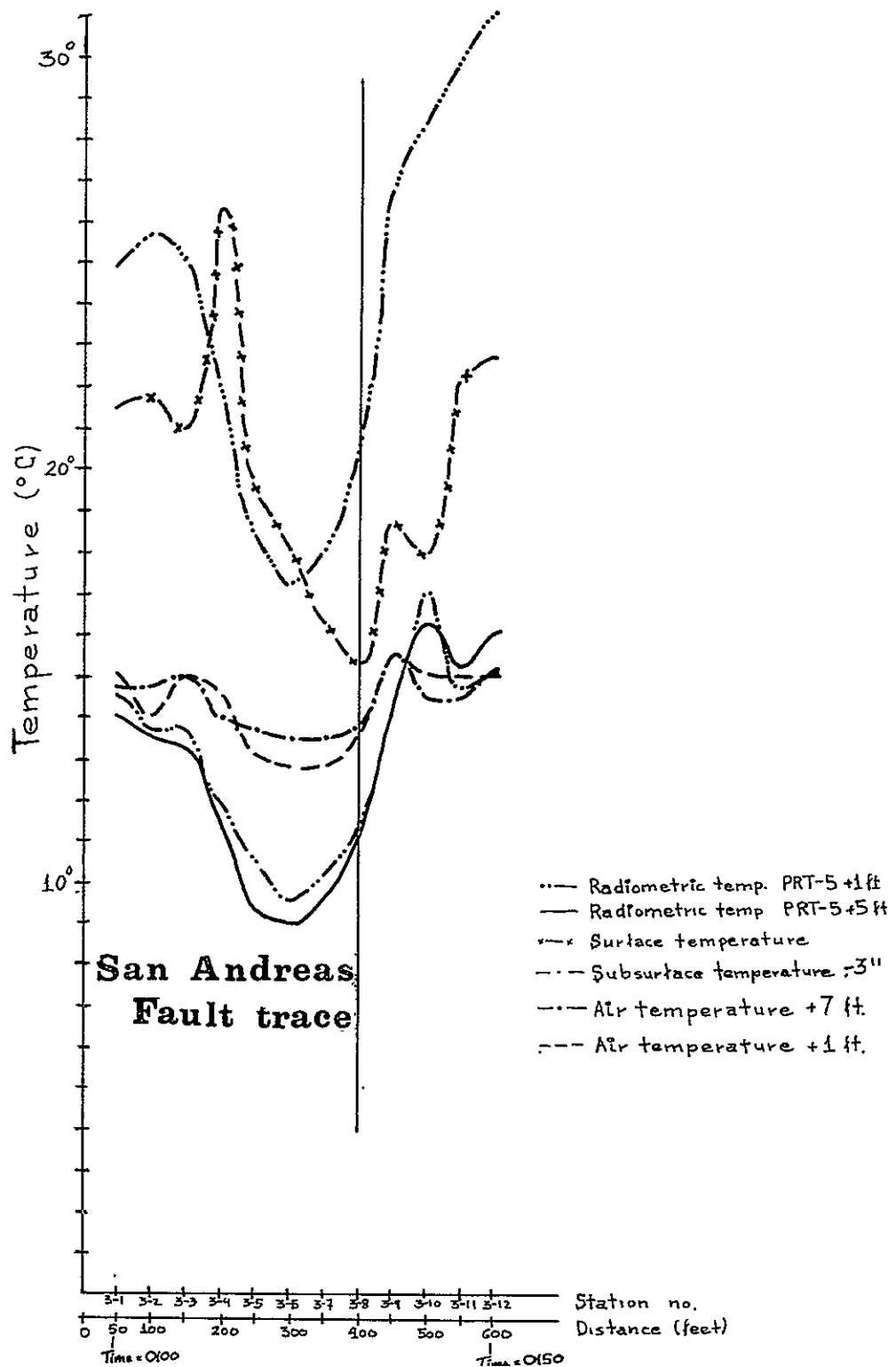
Figure 21. Temperature variations, smoothed curves, Site III

3. In general, there is a high correlation between all of the temper-
ature measurements.

XI. CONCLUSIONS

From the field data and results already presented, several con-
clusions can be drawn:

In the area investigated, there exists a definite thermal anomaly
across the San Andreas Fault zone as observed from the ground data and
thermal imagery. This anomaly is a function of many variables, includ-
ing topography, moisture content of the soil, surface conditions and
vegetative cover of the soil, as well as the atmospheric conditions,
humidity, and average daily temperature of the area. The observed
anomalies range in magnitude from 3° to 18° C, depending on the local
specific area being investigated and the type of instrument used.

Strong thermal anomalies not directly associated with the fault
also exist in the area. The prime example of this is the negative
anomaly found across Site II. Inspection of the imagery also indicates
that many other variations in temperature not associated with the fault
may be found. However, all of the these anomalies that were field
checked were found to be associated with topographic discontinuities.

The most important variable controlling ground temperature is the
moisture content of the soil. This is supported by the following
arguments:

1. Data collected on Site I shows a very strong negetative correlation
between ground temperatures and moisture content of the soil. The cor-
responding correlation coefficients of -0.57 to -0.67 are given in
Table V. The same high correlation was observed in the soil moisture
experiment as previously noted.

43

TABLE V: SELECTED CORRELATION MATRIX – SITE I

		A	B	C	D	E	F	G	H	I	J
A.	Radiometric Temp PRT-5, sweep	1.00									
B.	Relative Humidity (percent)	-0.53	1.00								
C.	Radiometric Temp PRT-5, 12 inches	0.73	-0.76	1.00							
D.	Radiometric Temp PRT-5, 60 inches	0.77	-0.80	0.91	1.00						
E.	Radiometric Temp PRT-10, 36 inches	0.65	-0.58	0.73	0.74	1.00					
F.	Contact Temp Surface	0.48	-0.53	0.46	0.48	0.47	1.00				
G.	Contact Temp -3 inches	0.63	-0.66	0.76	0.75	0.50	0.65	1.00			
H.	Air Temperature 12 inches	0.52	-0.64	0.66	0.73	0.62	---	0.42	1.00		
I.	Air Temperature 84 inches	0.61	-0.81	0.75	0.84	0.53	--	0.60	0.83	1.00	
J.	Moisture Content of soil (%)	-0.61	0.60	-0.62	-0.70	-0.57	-0.60	-0.64	-0.48	-0.70	1.00

No. of data stations = 41

44

TABLE VI. SELECTED CORRELATION MATRIX – SITE III

		A	B	C	D	E	F	G
A.	Relative Humidity (percent)	1.00						
B.	Radiometric Temp PRT-5, 12 inches	0.67	1.00					
C.	Radiometric Temp PRT-5, 60 inches	0.62	0.99	1.00				
D.	Contact Temp Surface	0.67	0.86	0.84	1.00			
E.	Contact Temp –3 inches	0.68	0.97	0.97	0.84	1.00		
F.	Air Temperature 12 inches	0.90	0.88	0.85	0.88	0.86	1.00	
G.	Air Temperature 84 inches	0.90	0.91	0.88	0.90	0.90	0.98	1.00

No. of data stations = 12

2. As may be seen from the photographs of the area, vegetation was more abundant in those areas, which later proved to have greater soil moisture content. We have not been able to prove which of the two factors, soil moisture or dead vegetative cover, is directly related with the lowered amount of infrared radiance. The soils of lower temperature and high moisture content correlate with the topographically-lower parts of the terrain, therefore increasing the chances of being closer to the water table and possibly decreasing the evaporation of water during the day because of "shadowing" effects of surrounding hills.

3. Cartwright (1968) states that soil moisture is one of the controlling factors of soil temperature. His values for thermal diffusivity of some soils show that moist soils and clay have a higher thermal diffusivity than do dry soils.

$$\alpha = K/C\rho$$

α = thermal diffusivity

K = conductivity

C = specific heat

ρ = density

α-values for very dry soils range from 0.002 (cgs units) to 0.003 while α-values for some wet soils range from 0.004 to 0.010. The thermal diffusivity of water at 0° C is 0.0013 and at 8° C is 0.0017. Assuming that the specific heat and density of the soils measured remain constant, the conductivity of the soils would be a direct positive function of the moisture content of the soil.

In general, the night-time temperatures at 3 inches depth were higher than surface temperatures. This implies a thermal gradient in the soil and, hence, a heat flow upwards (due to the daily solar loading). Variations of the gradient are shown in Figure 22 for each station. The average temperature gradient at Site I is 1.55° C/inch to a depth of 3 inches; the average gradient is 2.1° C/in. on the SW side of the fault and 1.2° C/in. on the NE side of the fault indicating either a lower thermal conductivity or higher heat flow for the SW side. Since the SW side has a lower moisture content, the thermal conductivity can be expected to be correspondingly lower. However, as no temperature measurements were taken at depths below the penetration of the diurnal wave, no assumptions concerning heat flow can be made.

Radiometric temperatures taken with the PRT-5 vary considerably from surface contact temperatures. The radiometric temperatures are lower by about 3° to 10° C than the contact temperatures, and about 1° to 6° C lower than air temperatures. The radiometric temperature measurements taken at 12 inches from the surface are consistently about 1° C higher than those taken at 60 inches from the surface. The only two variables which change in this system are the length of the air path and areal extent of the ground being observed. Since the temperature difference observed is consistent over most of the station-line, the change in viewing area would seem to be of no significance. Thus, the path length seems to be the critical variable in this difference. It seems probable that absorption by one of the gases in the atmosphere may be responsible for this effect. Of the major constituents
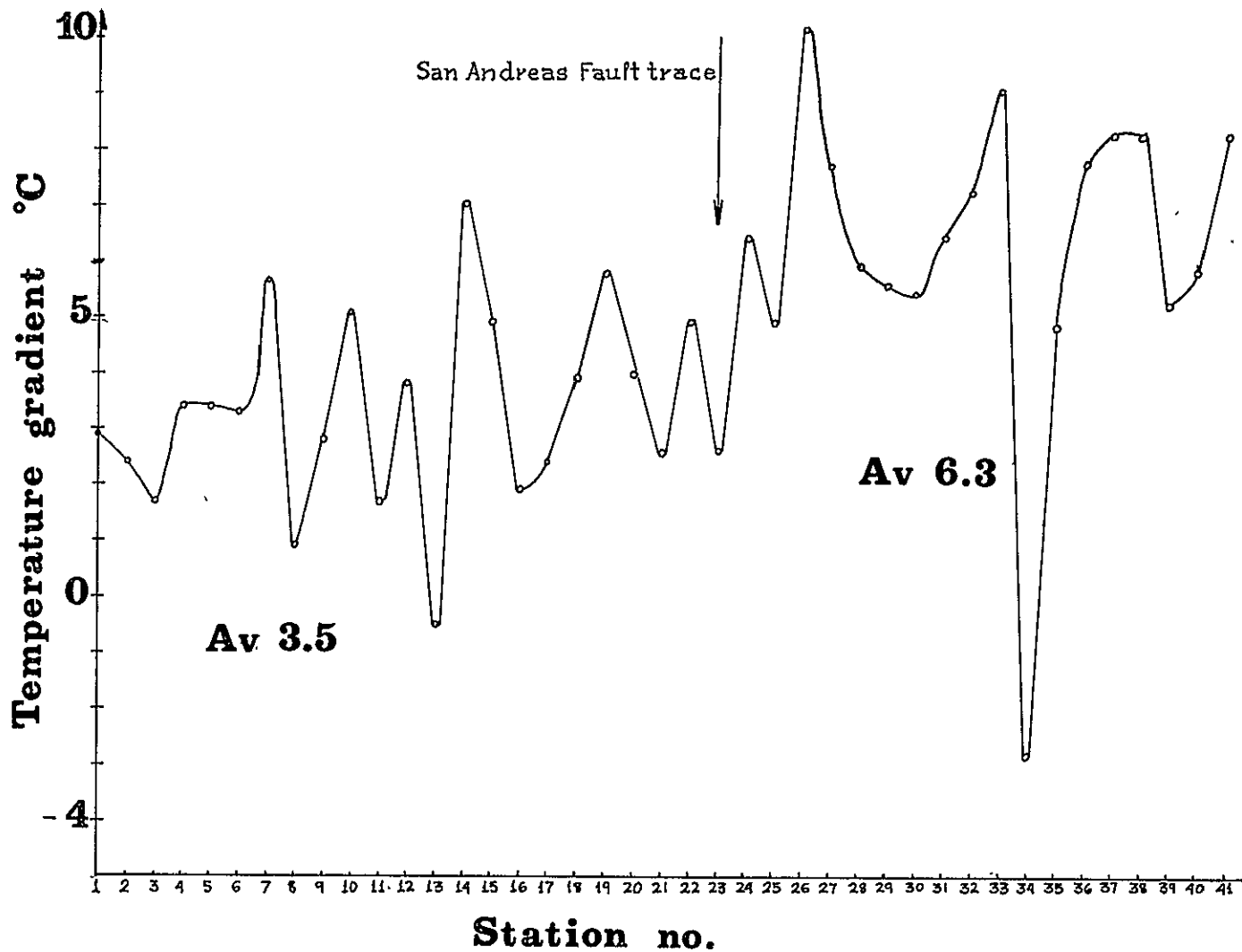
Figure 22. Soil thermal−gradient along station−line
Site I

in the atmosphere, only three have absorption bands in the 8 to 13 micron wavelength region - CO_2, O_3, and H_2O. CO_2 has a absorption band around 9.5 microns and water has numerous bands throughout the 8 to 14 micron region. Figure 23 shows the absorption spectra for various atmospheric gases. Since the difference between the measurements at 12 and 60 inches varied over the traverses, it would seem logical to assume that the absorber also varies over the traverse. The most likely candidate is the amount of precipitable water.

From the correlation coefficients given in Tables V and VI obtained by computer processing (as described in Appendix I), the following correlations are noted:

1) Variables with low correlation

    Radiometric temperature versus surface contact temperature (positive)

    Moisture content of soil versus air temperature 12 inches above ground (negative)

2) Variables with medium correlation

    Radiometric temperature versus air temperature 12 inches above ground (positive)

    Surface contact temperature versus subsurface contact temperature at -3 inches (positive)

    Surface contact temperature versus moisture content of the soil (negative)
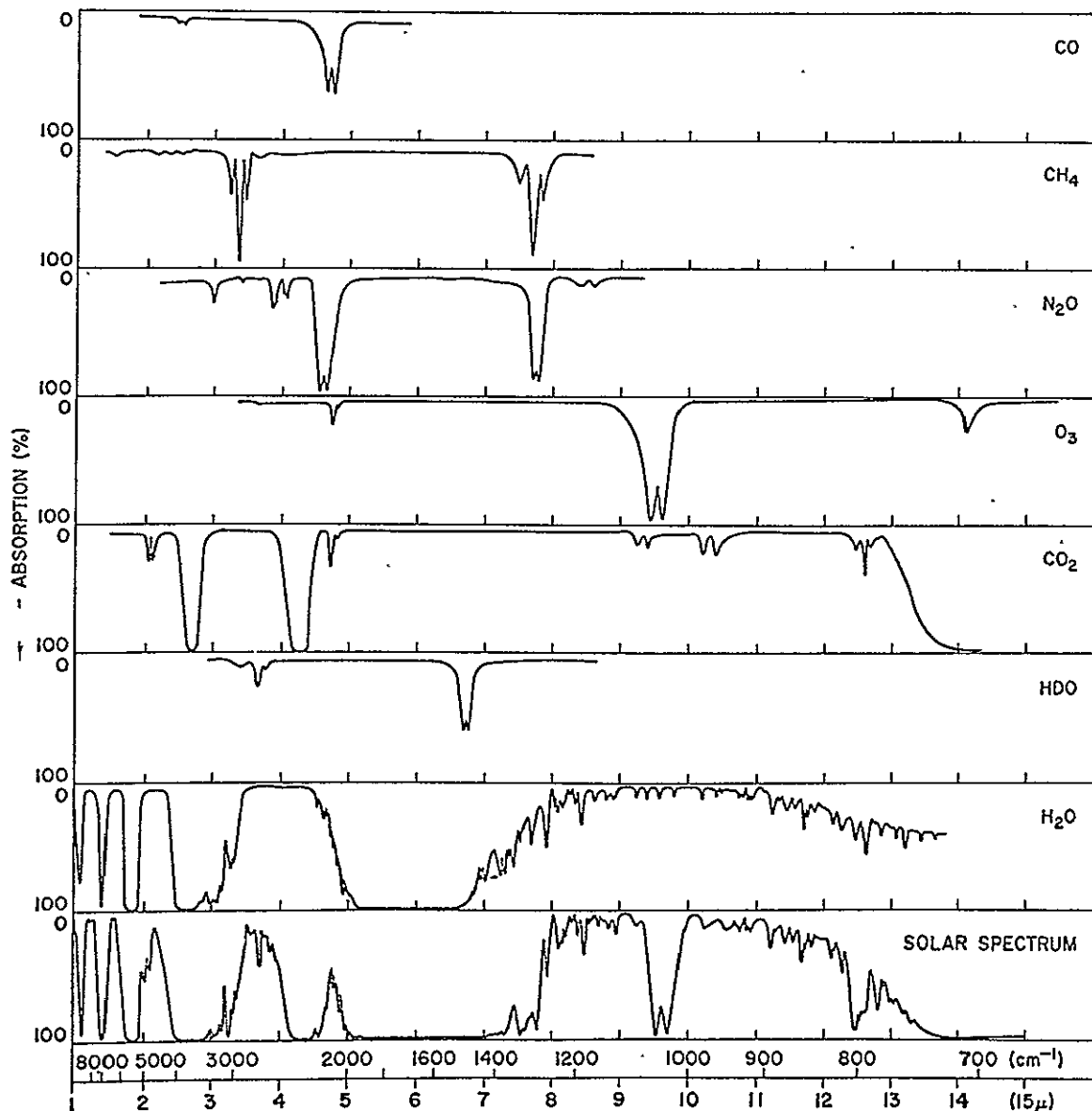
Figure 23 – Comparison of the near-infrared solar spectrum
with laboratory spectra of various atmospheric
gases. (After AFCRL Handbook of Geophysics
and Space Environments, Fig. 10-2, 1965.)

3) Variables with high correlation

Radiometric temperature versus subsurface contact temperature at

-3 inches (positive)

Radiometric temperature versus air temperature at 84 inches above

ground (positive)

Relative humidity versus air temperature at 12 and 84 inches above

ground (negative)

One source of error in the temperature measurements and resulting

correlations is the determination of the surface contact temperature.

Geiger (1965) shows experimental tautochrones that suggest that the

error in temperature T for a given error in depth X is much higher at

the surface than at depth. Since no field measurements of the tempera-

ture profiles below the surface deeper than the penetration of the diur-

nal wave were taken, we cannot determine the actual gradient, $\Delta T/\Delta X$.

Contact surface temperatures of bare ground measured at noon in a later

field study in Goldfield, Nevada, show no difference from radiometric

temperature while the same measurements taken at predawn do show a dif-

ference in radiometric temperature and surface contact temperature. At

present this deviation is unexplainable, but some study on methods of

the determination of the contact surface temperature of soils covered

with sparse, dead vegetation should be undertaken.

Previous literature (Wallace and Moxham, 1967) suggests that many

negative thermal anomalies in this and other areas may be directly

attributed to the presence of tumbleweed. Data gathered in this study

showed that tumbleweed did give an anomaly, but these anomalies were

not consistently positive or negative. Tumbleweed in the bottom of

51

depressions uniformly gave negative anomalies; however, tumbleweed in other places often gave a positive anomaly. It is our conclusion that a) tumbleweed acts as a thermal insulator, i.e., it tends to remain warm in areas which normally give positive anomalies and tends to remain cool in areas which normally give negative anomalies, and b) it is merely a coincidence that tumbleweed is associated with some of the strong thermal anomalies noticeable on the imagery and sensed in the field. These strong thermal anomalies tend to appear in topographically lower areas and likewise tumbleweed will tend to migrate to these same topographically low areas due to gravity (and lower wind). While the insulating effect of the tumbleweed may tend to accentuate the negative thermal anomaly, that same anomaly is present regardless of the presence of the tumbleweed.

The Barnes PRT-10 Infrared Field Thermometer proved to be somewhat of a disappointment in actual field use. It required constant calibration as it tended to drift quite badly. The placement of the calibration knob was such that it was easily moved during use, causing erroneous changes in calibration. In addition the PRT-10 gave consistently higher values than did the PRT-5, as discussed previously. However, despite all of these difficulties, the PRT-10 did detect approximately the same relative anomalies as did the PRT-5. If it could be stabilized and ruggedized for field use, it could be of value.

Smoothing of the data is of immense importance since it shows large-scale regional anomalies much more clearly than does the raw field data. However, the raw data is useful for showing detailed

localized anomalies and correlations of different variables and instruments. Smoothing can tend to shift minima and maxima and thus the smoothed and raw data should be presented to eliminate erroneous assumptions. Different smoothing formulae should be used to determine which present the most useful information.

XII. REFERENCES

Brown, R. D., Jr. and Wallace, R. E., 1968. Current and Historic
Fault Movement along the San Andreas Fault between Paicines and Camp
Dix, Cal.; in Proceedings of Conference on Geologic Problems of San
Andreas Fault System. Stanford University Pub., Geol. Scis., Vol. XI,
pg 22.

Cartwright, Keros, 1968, "Temperature Prospecting for Shallow Glacial
and Alluvial Aquifers in Illinois," Illinois State Geological Survey,
Circular, 433.

Deer, W. A., Howie, R. A., and Zussman J., 1962, "Rock-Forming Minerals,"
Vol. 3, Sheet Silicates, Longmans, Green and Co. Ltd., London, England.

Dibblee, T. W., Jr., 1968, "Regional Geologic Map of San Andreas Fault
from Cholame Area to Cuyama--Maricopa Area," USGS, unpublished map,
National Center for Earthquake Research.

Gates, D. N., 1964, "Characteristics of Soil and Vegetated Surfaces to
Reflected and Emitted Radiation," Symposium Remote Sensing of Environ-
ment, 3d, Michigan Univ., Ann Arbor, Infrared Physics Lab., Proc.,
pp. 573-600.

Geiger, R., 1965, The Climate Near the Ground, Harvard University Press.
Cambridge.

Howell, J. V. et al., 1960, Glossary of Geology and Related Sciences.
Am. Geol. Inst., Washington, D.C.

Stingelin, R. W., 1968, "Operational Airborne Thermal Imaging Surveys,"
Geophysics.

Wallace, R. E., and Moxham, R. M., 1967, "Use of Infrared Imagery in
Study of the San Andreas Fault System, California," Geological Survey
Research, 1967, U.S.G.S. Professional Paper, 575D, pp. D147-D156.

Wolfe, W. L., et al., 1965. Handbook of Military Infrared Technology.
Office of Naval Research, Dept. of the Navy, Washington, D.C.

APPENDIX I

A. Data Processing

A FORTRAN IV computer program, IRANAL, was written to compile and plot all of the data obtained. It was written for use with the Stanford IBM 360/67 computer system. The input data is punched on cards and read into the processor. Output consists of a listing of the original input data--lists of one variable versus another variable, graphical plots of original data versus station location for each station line, and "smoothed" graphical plots of the original data using a nine term "smoothing formula." A list of the original compilation and output is included in this appendix.

IRANAL can handle up to 500 station locations for each station line. Input is as follows:

FIRST CARD - N, number of stations in the station line must be entered in the first three columns.

SECOND CARD - This begins a series of data cards, each of which represents one station. Data card format is as follows:

COLUMN	VARIABLE
1-4	SITENO, station identification number
5	blank
6-9	DAY, date
10-11	blank
12-15	TIME, time on 24-hour system
16-17	blank

18-21	SWEEP, radiometric temperature from swept reading ("sweep")
22-23	blank
24-26	PHUMID, percent relative humidity
27-28	blank
29-32	WINDV, wind velocity in mph.
33-34	blank
35-38	PRT-51, radiometric temperature of PRT-5, 12 inches from ground
39-40	blank
41-44	PRT-55, radiometric temperature of PRT-5, 60 inches from ground
45-46	blank
47-48	PRT103, radiometric temperature of PRT-10, 36 inches from ground
49-50	blank
51-54	CT1, contact temperature of surface soil
55-56	blank
57-60	CT2, contact temperature of soil at 3 inches depth
61-62	blank
63-66	AT1, air temperature, 84 inches from ground
67-68	blank
69-72	AT2, air temperature, 12 inches from ground
73-74	blank
75-79	MOIST, moisture content of soil (%)

Output from IRANAL is as follows:

1. Listing of all input data

2. Listing of time versus all variables from future plotting

3. Listing of humidity and moisture content of the soil versus all variables for future plotting

4. Listing of all radiometric temperatures for future comparison

5. Listing of radiometric temperatures versus contact temperatures

6. Graphs of rough and "smoothed" data of all variables versus station number.

The smoothing of the rough data is accomplished.by the following smoothing formula:

$SMOOTH (I) = 59/331 ROUGH (I) + 54/231 (ROUGH (I-1) + ROUGH (I + 1) + 39/231 (ROUGH (-I-2) + ROUGH (I + 2)) + 14/231 (ROUGH (I-3) + ROUGH (I + 3)) - 21/231 (ROUGH (I-4) + ROUGH (I + 4))$

This is a weighted, running-average type of smoothing formula. Since it requires four values on either side of the value being smoothed, the first and last four values in each graph are not smoothed and are represented by the original rough data.

B. <u>CORREL</u>

CORREL is a product-moment correlation coefficient computer program written in FORTRAN IV for use with an IBM 360/67 computer system. It makes use of the subroutine CORRE in the IBM Scientific Subroutine Package. Data, fed into CORREL, are all cross-correlated with one another. The most important output is a table of correlation coeffients calculated for all pairs of variables.

A list of the original compilation is included in Appendix C.

Input to CORREL is as follows:

FIRST CARD - NVAR AND NOBS, the number of variables and number of observations respectively, must be entered in that order in the first three and second three columns of the first card.

SECOND CARD - This begins a series of NOBS data cards. Data card format is as follows and with variable names referring to the same variables as in IRANAL 2.

COLUMN NUMBER	VARIABLE
1 – 4	SITENO
5 – 8	ALT
9 – 12	TIME
13	blank
14 – 15	HUMBEN
16	blank
17 – 20	HUMHON
21	blank
22 – 23	WINDV
24	blank
25 – 28	PRT51
29	blank
30 – 33	PRT55
34	blank
35 – 38	PRT51R
39	blank
40 – 43	PRT55R
44	blank
45 – 48	PRT5S
49	blank
50 – 53	SUBST
54	blank
55 – 58	WBT
59	blank
60 – 63	DBT

64	blank
65 - 67	VPTB
68	blank
69 - 70	ATH
71	blank
72 - 74	VPTH
75	blank
76 - 80	MOIST

Output from CORREL is as follows:

1.) Listing of MEANS for each variable

2.) Listing of STANDARD DEVIATIONS for each variable

3.) Listing of SUM OF X-PRODUCT OF DEVIATION FROM MEANS for all variables

4.) Correlation Matrix in which each variable has been cross-correlated with every other variable.

The significance of these correlation coefficients may be determined for each traverse by use of Figure 26.

APPENDIX II

For each of the sites the following data was taken.

		Site I	Site II	Site III
1)	Site number - the first digit refers to the site number and the following numbers refer to the station number	X	X	X
2)	Date	X	X	X
3)	Time - 24 hours system	X	X	X
4)	Relative humidity	X	X	X
5)	Sky conditions (cloudy, clear, etc.)	X	X	X
6)	Wind velocity (miles/hour)	X	X	X
7)	Radiometric temperature PRT-5, 12 inches from ground surface	X	X	X
8)	Radiometric temperature PRT-5, 60 inches from ground surface	X	X	X
9)	Radiometric temperature PRT-10, 36 inches from ground surface	X	–	–
10)	Sky temperature	X	X	X
11)	Contact temperature of soil surface	X	–	X
12)	Contact temperature of soil at 3 inches depth	X	X	X
13)	Air temperature 12 inches from ground	X	X	X
14)	Air temperature 84 inches from ground	X	–	X
15)	Notes on interesting or unique features	X	X	X
16)	Soil sample for moisture analysis	X	–	–

DISTRIBUTION LIST

USGS	No. of copie
Max Crittenden	1
Bob Alexander	1
Harry Smedes	1
R. W. Fary	1
W. H. Hemphill	1
Gordon Greene	2
C. V. Robinove	1
K. Watson	1
S. J. Gawarecki (plus reproducible original	6
Wm. A. Fischer	1
R. Ashley	1
R. Moxham	1

NASA-WASHINGTON	
Arch Park	1
T. A. George	1
J. Koutsandreas	1

NASA-HOUSTON	
Tom Barnett	1
J. E. Dornbach	1
Charles M. Grant	1
R. Piland	1
Ed Seitler	1
Retha Shirkay (Technical Information Dissemination Branch)	4
John Wheeler	1
Larry Hoover	1

NASA/MSFC-Huntsville	
J. Fountain	1

NASA-GODDARD	
Warren Hovis	1
William Nordberg	1

USNOO	
H. Yotko	1

OTHERS

Len Bowden	1
Branner Library	1
R. N. Colwell	1
Roger Holmes	1
Dave Landgrebe	1
R. K. Moore	1
Bob Peplies	1
Jack Quade	1
Ralph Shay	1
Dave Simonett	1
Don Walsh	1
E. W. T. Whitter	1
L. T. Grose	1
Keenan Lee	1
R. B. MacDonald	1
V. Myers	1
R. Campbell	1
F. Querol-Suñé	1